Physics – Uspekhi **41** (9) 865 – 884 (1998)

REVIEWS OF TOPICAL PROBLEMS PACS numbers: 43.35.Cg, 64.60.Ht, **75.50.y**

Ultrasonic studies of the critical dynamics of magnetically ordered crystals

I K Kamilov, Kh K Aliev

Contents

Abstract. The current state of ultrasonic research of dynamic critical phenomena in magnetically ordered crystals is reviewed. Based on relevant theoretical concepts, the conclusion is drawn that the experimental data on ferro-, ferri-, and antiferromagnetic materials in both the hydrodynamic and critical regions can be described in terms of the dynamic scaling concept and the theory of interacting modes. The influence of a magnetic field on the dynamics of critical fluctuations of magnetization and spin-energy density is discussed.

1. Introduction

The progress achieved in recent years in the understanding of critical phenomena in magnetically ordered crystals [1 – 6] has largely been due to theoretical and experimental works devoted to studying the critical dynamics of condensed media. The existing concepts of the time evolution of critical fluctuations were developed in the framework of the theory of interacting modes and dynamic scaling. These research directions, although being developed independently from one another and based on completely different ideas, in each particular case lead to predictions that agree well.

The first direction originates from the classical works of Landau and Khalatnikov [7] and Van Hove [8], who gave a theoretical justification of the phenomenon (long since noticed by experimenters) of a sharp increase in the time required for the system to pass from a nonequilibrium to equilibrium state as a critical point is approached. These theories qualitatively explained many experimental facts but ignored the divergence of transport coefficients. Fixman was the first (see, e.g., Ref. [8]) who tried to allow for the divergence of transport coefficients; he believed that the long-range spatial correlations predicted by the Ornstein – Zernike theory [1] intensify fluctuations, which in turn can lead to anomalous changes in the transport coefficients.

This fruitful idea was further developed in Refs [8, 9] where it was shown in terms of time correlation functions that the divergence of transport coefficients is caused by the decay of one hydrodynamic mode into several hydrodynamic modes (theory of interacting modes).

In parallel with the theory of interacting modes, a purely phenomenological approximation was also developed, based on the concepts of Ferrela et al. (see Ref. [8]), who extended the ideas of the static scaling theory to dynamic phenomena. Later, this theory was generalized by Halperin and Hohenberg [10] and applied to particular systems.

The relation between these two approaches was found by Kawasaki [8], who showed that instead of hydrodynamic modes, a set of dynamic variables can be introduced, whose dynamics has a characteristic spectrum of frequencies predicted by dynamic scaling.

A natural result of the theoretical studies in critical dynamics was the use of the method of the renormalization group and Wilson's ε expansion [11] to study dynamic phenomena [12], which allowed the calculation of the dynamic critical exponent z for concrete models and the establishment of factors affecting its numerical values; the value of z proved to depend not only on the spatial dimensionality d, the number of the degrees of freedom of the order parameter n, and the nature of the ordering

I K Kamilov Institute of Physics, Russian Academy of Sciences, Dagestan Science Center, ul. Yaragskogo 94, 367003 Makhachkala, Russia
Tel. (8-8722) 62 89 60
Kh K Aliev Dagestan State University,
ul. M. Gadzhieva 43a, 367025 Makhachkala, Russia
Tel. (8-8722) 67 59 65

Received 4 June 1997, revised 24 March 1998
Uspekhi Fizicheskikh Nauk **168** (9) 953 – 974 (1998)
Translated by S N Gorin; edited by S D Danilov

interaction, but also on the satisfiability of the laws of conservation of the characteristic energy and order parameter.

The critical dynamics of magnetically ordered crystals, especially ferromagnets, exhibits extremely varied and complex features, which are caused by the necessity of taking into account, apart from the exchange interactions, weak relativistic interactions. The most significant of these are dipolar interactions, whose role increases on approaching the critical point. As a result, the critical region turns out to be divided into the exchange and the dipole regions [13 – 15]. In the exchange region, as the experiments performed on ferromagnets such as EuO, EuS, Ni, Fe indicate, predictions of the theory of interacting modes and dynamic scaling are valid [13 – 15]. In the dipole region, the theory predicts two variants of dynamics: the conventional and a rigid [13 – 16]. The experimental situation is still unclear because of the discrepancies in the existing data obtained by the methods that allow studying two-spin correlations (dynamic susceptibility, EPR, light and neutron scattering, etc.).

In the entire critical region of magnetically ordered crystals, the decisive part in the formation of critical dynamics belongs to four-spin correlations, which can be studied by ultrasonic methods [17, 18]. The advantage of ultrasonic methods is not only the possibility of studying four-spin correlations, but also the fact that they permit simultaneous measurements of both static and dynamic properties. Measurements of sound velocities give information on the equilibrium properties, while measurements of sound attenuation yield information on the dynamic properties of a material. The interest in ultrasonic investigations is additionally increased due to the fact that the elastic waves affect the spin system via the spin – phonon interaction of magnetostrictive origin rather than directly. Depending on the nature of the exchange interaction, three types of interaction between sound waves and spin system are distinguished [19]. In magnetic metals, where both localized 3d and 4f electrons and itinerant s electrons are involved in the exchange interaction, the interaction with spin fluctuations is predominantly quadratic. In magnetic insulators, the exchange interaction is short-range and the sound waves largely interact with fluctuations of the spin-energy density, which yields a linear relation to the spin Hamiltonian. In both insulating and metallic magnetically ordered crystals, a linear relation with the order parameter exists below the critical temperature, which leads to the well-known mechanism of anomalous propagation of sound waves called the Landau – Khalatnikov mechanism. The first two types of interaction result in a fluctuation mechanism and the third type yields a relaxation mechanism.

The strength of the singularity of the attenuation coefficient α_k and the propagation velocity v_L when the fluctuation mechanism is operative are determined by the nature of the exchange interaction, magnetic ordering, and anisotropy. In particular, in magnetic insulators, where the exchange interaction is short-range, the critical attenuation exhibits only a weak singularity, because the sound absorption is due to the fluctuations of the spin-energy density, which decay via slow spin – lattice relaxation [18 – 21]. In the case of long-range interaction, the singularity is much stronger, since the main contribution to the critical attenuation comes from the fluctuations of the order parameter, while the relaxation is due to the spin – spin interaction [18 – 23].

The theory of critical attenuation of sound waves in magnetic metals, which was developed by Kadanoff [9, 20] and Kawasaki [19] for the hydrodynamic region $\omega\tau \ll 1$ (ω is the angular frequency, and τ is the relaxation time), was confirmed experimentally in ultrasonic investigations performed on Ni [24 – 26], MnP [27], and rare-earth metals [18]. It was shown in later theoretical works [19, 28 – 31] that in both the hydrodynamic and critical ($\omega\tau \geqslant 1$) regions, the coefficient α_k is described by a simple scaling function of the variable $\omega\tau$. The experimental investigations performed on three-dimensional Heisenberg ferromagnets Gd [18] and MnP [27, 31] and on a two-dimensional Ising antiferromagnet Rb_2CoF_4 [29, 30] confirmed the validity of the concepts of dynamic scaling.

Although critical dynamics have been studied by ultrasonic methods in numerous works of both foreign and domestic authors, no reviews have been published in recent years devoted to systematizing the experimental and theoretical studies of the propagation velocity and attenuation of ultrasonic waves in either the hydrodynamic or critical region. The last review concerning this question was published in 1977 [19] and, naturally, does not reflect the modern state of the problem of investigation of critical dynamics of magnetically ordered crystals by ultrasonic methods.

The work presented here is aimed to fill this gap. It generalizes experimental and theoretical investigations in the field of propagation of ultrasound in the critical region not only in ferromagnets and antiferromagnets, but also in ferrimagnets, which are substances that are close to insulators in electrical properties, to ferromagnets in magnetic properties, and to antiferromagnets in spin-ordering effects (properties that first were studied by the authors of this review [32 – 42]).

2. Mechanism of the spin – lattice interaction

In magnetically ordered crystals, the anomalous propagation of sound waves near the Curie (Néel) temperature is controlled by spin – lattice interactions which have a magnetostrictive origin. In this temperature range the interaction between the spin system and the lattice is implemented by two mechanisms: single-ion (linear-magnetostrictive) and two-ion (volume-magnetostrictive) [18].

When considering these mechanisms, the Hamiltonian of the system is written in the form [43]

$$\mathcal{H} = \mathcal{H}_0 + \mathcal{H}_1 + \mathcal{H}_2\,, \tag{2.1}$$

where

$$\mathcal{H}_0 = \sum_{\mathbf{k}} \hbar\omega_{\mathbf{k}}^0 b_{\mathbf{k}}^* b_{\mathbf{k}} - \sum_{\alpha}\sum_{i,j} J_{i,j}^{\alpha} S_i^{\alpha} S_j^{\alpha} + g\mu_B H \sum_i S_i^z \tag{2.2}$$

is the Hamiltonian of noninteracting spins S_i and phonons with frequency $\omega_{\mathbf{k}}^0$ and polarization vector $\mathbf{e}_{\mathbf{k}}$; $b_{\mathbf{k}}$ and $b_{\mathbf{k}}^*$ are the operators of annihilation and creation of phonons, respectively. From here below, J is the exchange integral, S is the spin number, g is the Landé factor, μ_B is the Bohr magneton, and $\hbar$ is Planck's constant. The latter term in $\mathcal{H}_0$ represents the Zeeman energy for the case $H \parallel z$. $\mathcal{H}_1$ and $\mathcal{H}_2$ are the spin – phonon interactions of first and second orders with respect to the phonon amplitudes, i.e., the volume-magnetostriction and linear-magnetostriction interactions,

respectively. They are determined by the expressions

$$\mathcal{H}_1 = \sum_{\mathbf{k}} \sqrt{\frac{\hbar}{2\rho V \omega_{\mathbf{k}}^0}}\,(b_{\mathbf{k}} + b_{\mathbf{k}}^*) U_{\mathbf{k}}^{(1)}\,, \tag{2.3}$$

$$\mathcal{H}_2 = \sum_{\mathbf{k}} \sum_{\mathbf{k}'} \frac{\hbar}{2\rho V} (\omega_{\mathbf{k}}^0 \omega_{\mathbf{k}'}^0)^{-1/2} (b_{\mathbf{k}} b_{-\mathbf{k}'} + b_{-\mathbf{k}}^* b_{\mathbf{k}'}^* + b_{\mathbf{k}} b_{\mathbf{k}'}^* + b_{-\mathbf{k}}^* b_{-\mathbf{k}}) U_{\mathbf{k}\mathbf{k}'}^{(2)}\,. \tag{2.4}$$

Here

$$U_{\mathbf{k}}^{(1)} = -\sum_{i,j} \left[\exp(\mathrm{i}\mathbf{k}\mathbf{R}_i) - \exp(-\mathrm{i}\mathbf{k}\mathbf{R}_j)\right] \mathbf{e}_{\mathbf{k}} \sum_{\alpha} \frac{\partial J_{ij}^{\alpha}}{\partial \mathbf{R}_i} S_i^{\alpha} S_j^{\alpha}\,, \tag{2.5}$$

$$U_{\mathbf{k}\mathbf{k}'}^{(2)} = -\frac{1}{2} \sum_{i,j} \left[\exp(\mathrm{i}\mathbf{k}\mathbf{R}_i) - \exp(\mathrm{i}\mathbf{k}\mathbf{R}_j)\right] \times \left[\exp(-\mathrm{i}\mathbf{k}'\mathbf{R}_i) - \exp(-\mathrm{i}\mathbf{k}'\mathbf{R}_j)\right] \times \mathbf{e}_{\mathbf{k}} \mathbf{e}_{\mathbf{k}'} \sum_{\alpha} \frac{\partial^2 J_{ij}^{\alpha}}{\partial \mathbf{R}_i\, \partial \mathbf{R}_j} S_i^{\alpha} S_j^{\alpha}\,, \tag{2.6}$$

where ρ is the density. As can be seen from (2.3)–(2.6), the change in the length of the vector $\mathbf{R}_i$ that links two lattice sites with spins S_i is a first-order quantity with respect to elastic stresses for longitudinal waves, and a second-order quantity for transverse waves propagating along the symmetry axes of the crystal. In other words, this means that the propagation of longitudinal waves results in a volume deformation, whereas transverse waves cause shape deformation.

The very value of the critical attenuation at a fixed frequency depends on the values of the spin–phonon interaction constants. These constants cannot be calculated theoretically. The volume-magnetostrictive interaction constant B_{V} can be evaluated from the displacement of the Curie point under the action of hydrostatic pressure, the anomaly of the thermal expansion coefficient, and the true volume magnetostriction. The preferred method is the estimation of B_{V} from the dependence of the exchange interaction on pressure (volume). In this case, B_{V} is expressed through the exchange-integral derivative with respect to the interatomic distance a:

$$B_{\mathrm{V}} = Na\,\frac{\partial J}{\partial a} = \frac{3N_{\mathrm{A}}\rho}{M}\,J\gamma_{\mathrm{m}}\,, \tag{2.7}$$

where $\partial J/\partial a$ is estimated from the displacement of the Curie point under the action of a hydrostatic pressure; N is the number of atoms per unit volume;

$$\gamma_{\mathrm{m}} = \frac{\partial \ln J}{\partial \ln V} = -\frac{1}{B_{\mathrm{T}}}\,\frac{\partial \ln T_{\mathrm{c}}}{\partial P} \tag{2.8}$$

is the Grüneisen constant; and B_{T} is the compressibility.

The linear-magnetostrictive interaction constant $B_{\perp}$ is determined as

$$B_{\perp} = 2.4 C_{44} \lambda_0\,, \tag{2.9}$$

where C_{44} is the elastic constant and λ_0 is the magnetostriction at $T = 0$ K.

When estimating the magnetoelastic constants B_{V} and $B_{\perp}$ for magnetic insulators, Bloch showed [44] that the energy of volume interaction varies as the 10/3 power of volume and, consequently, $\gamma_{\mathrm{m}} = 10/3$. Later, Samara and Jiardini [45] verified this law. This conclusion is also confirmed by our data on thermal expansion. In particular, the values of the Grüneisen constant γ_{m} obtained from the slopes of the $\Delta\alpha_{\mathrm{H}} = f(\Delta C_{\mathrm{H}})$ dependences coincide within 10% with the above estimates.

When estimating B_{V} in the rare-earth metal Gd, it should be remembered that the dependence of the exchange integral on the interatomic spacing has different signs for the hexagonal axis and the basal plane and that the Grüneisen constants for the a and c axes differ at above and below T_{c} [46]. For this reason, the B_{V} values for Gd are estimated from the average value of γ_{m}.

The B_{V} and $B_{\perp}$ constants calculated by (2.7) and (2.9) are given in Table 1. The table also lists the data on the Curie (Néel) temperatures, anisotropy parameters, and Grüneisen constants.

Table 1. Spin–phonon interaction constants.

Material	Curie (Néel) temperature	Anisotropy parameter	γ_{m}	B_{V}, 10^7 J m^{-3}	$B_{\perp}$, 10^7 J m^{-3}
Gd	290.1	5×10^{-4}	2.00	9000	20
Tb	227.6	-0.4	1.39	7500	1280
Dy	177.3	-0.3	1.30	6000	1440
Ho	132.1	-7×10^{-2}	1.08	2200	460
MnP	290.5		—	3200	—
Ni	630.0	$\sim 10^{-4}$	1.20	2360	—
Rb_2CoF_4	103.2	0.55	—	—	—
EuO	69.4	4×10^{-4}	3.33	2700	40
$RbMnF_3$	83.0	5×10^{-6}	3.13	—	0.2
MnF_2	67.3	3×10^{-2}	3.33	1300	
Fe_3O_4	858.0	10^{-4}	3.33	281.5	20†
$Y_3Fe_5O_{12}$	548.25	10^{-5}	3.13	151.2	1.28
$Gd_3Fe_5O_{12}$	560.0	10^{-5}	3.20	160.5	1.5

† The values of the interaction constants for the ferrimagnets have not been normalized with respect to the reduced magnetization.

Based on an analysis of the interaction constants given in Table 1, we may conclude that in all magnetically ordered crystals, including ferrimagnets with spinel and garnet structures, anomalies of the velocity and attenuation of ultrasonic waves must be observed. From comparison of B_{V} and $B_{\perp}$, it follows that the main mechanism of spin–phonon coupling in virtually all the crystals that were studied is magnetostrictive. Therefore, it is only anomalies in the behavior of longitudinal waves that are expected near the Curie point. In magnetite and rare-earth metals such as Tb, Ho, and Dy, the significant contribution of the linear-magnetostrictive interaction to the spin–phonon interaction can also result in anomalies for transverse waves, but only if the conditions given in the following section are fulfilled.

3. Sound propagation near the Curie point

When experimentally studying the propagation of ultrasonic waves, the first parameters to be measured are the propagation velocity and the attenuation coefficient and they are measured not only near the phase-transition temperature but also over a wide temperature range. In all the magnetically ordered crystals that were studied, anomalies characteristic of second-order phase transitions were revealed near the critical temperature.

As is seen from Figs 1–4, the propagation velocity v_{L} or the velocity shift $\Delta v/v_0$ passes through a minimum, and the attenuation coefficient $\alpha_{\mathbf{k}}$ goes through a maximum. The

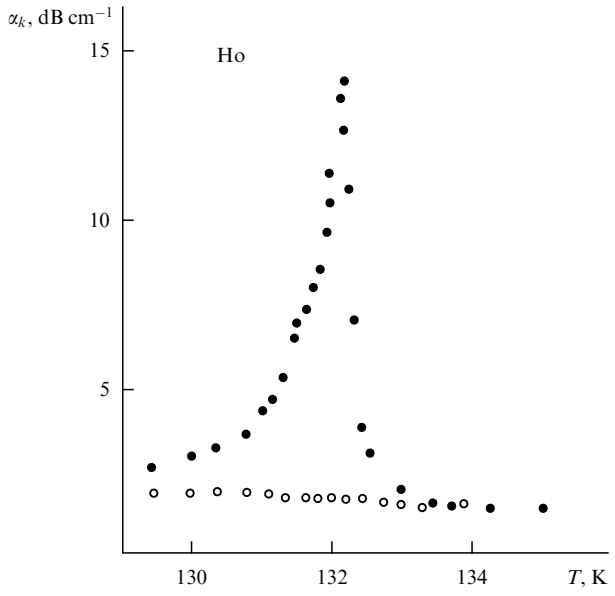

Figure 1. Attenuation of ultrasonic waves of frequency 50 MHz along the *c* axis of holmium [48]: •, longitudinal; ○, transverse.

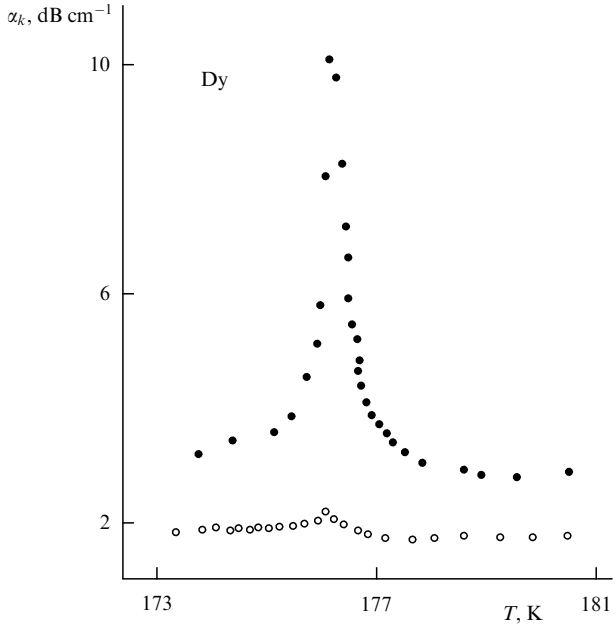

Figure 2. Attenuation of ultrasonic waves of frequency 50 MHz along the *c* axis of dysprosium [48]: •, longitudinal; ○, transverse.

temperatures at which the anomalies of $\alpha_{\mathbf{k}}$ and v_{L} are observed do not coincide and are displaced toward lower temperatures relative to T_{c} (see Figs 3 and 4).

Another characteristic feature of magnetically ordered crystals is that not only their attenuation coefficient increases in magnitude but its maximum shifts toward lower temperatures. The ultrasound propagation velocity only weakly depends on frequency. However, in the immediate vicinity of T_{c}, the velocity depends on the frequency strongly.

These and some other features of the propagation of ultrasonic waves in magnetically ordered crystals can be illustrated using the substances studied as examples.

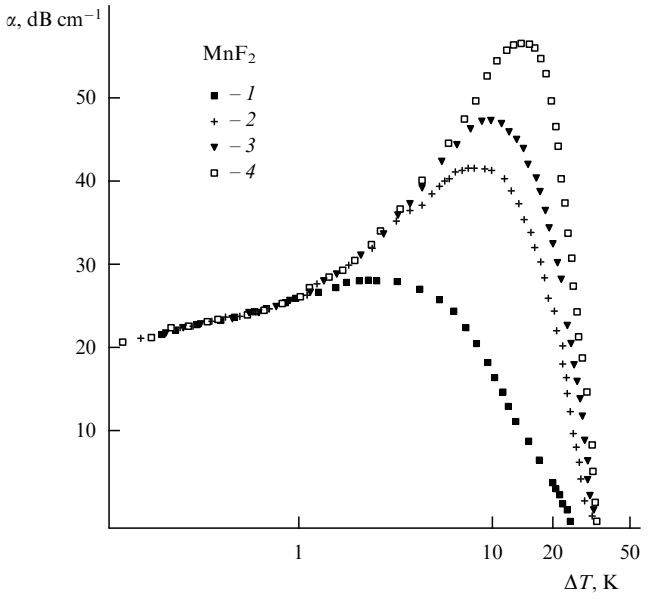

Figure 3. Attenuation of longitudinal ultrasonic waves in the ordered phase of MnF_2 [56] for the propagation direction [001] at several frequencies: *1*, 200; *2*, 500; *3*, 720; and *4*, 1000 MHz.

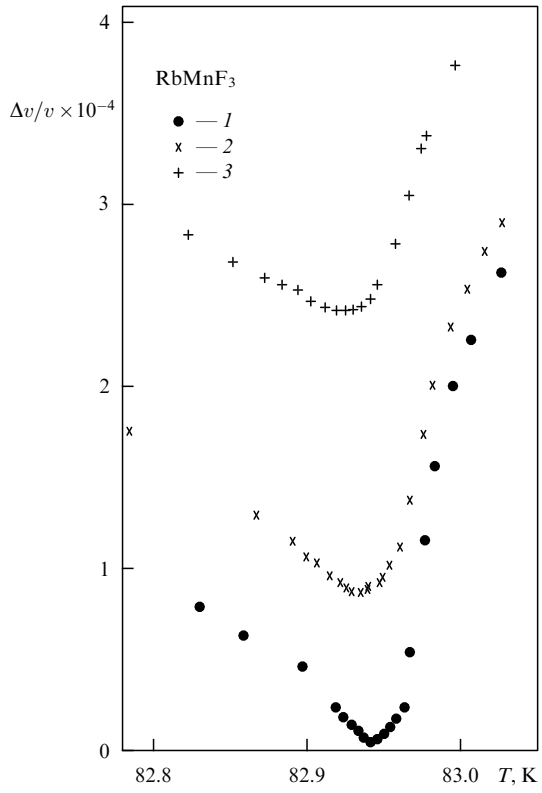

Figure 4. Propagation velocity of ultrasonic waves in $RbMnF_3$ [55] for the propagation direction [001] at several frequencies: *1*, 30; *2*, 90; and *3*, 150 MHz.

The experimental studies performed on ferromagnets such as Gd [18, 47–50] and MnP [27, 31, 51] and on antiferromagnets MnF_2 [52–58] and $RbMnF_3$ [18, 21, 55–58] show that longitudinal waves exhibit critical attenuation, whereas for transverse waves, no anomalies occur at the Curie

(Néel) point or they are much less than for the longitudinal waves. This can be explained as follows [58]. The longitudinal waves are related to the spin system through the modulation of the exchange interaction by strain fields; for the transverse waves, this interaction is absent. The transverse waves are related to spins through an anisotropic magnetostrictive interaction, which is much weaker than the isotropic exchange interaction in crystals where the magnetic ions are in the S state. Since the attenuation coefficient α_k is proportional to the square of the spin–phonon interaction constant, the values of α_k for the transverse waves are much less than for the longitudinal waves. As is shown by magnetostriction investigations of rare-earth metals, whose atoms are not in the S state, the constants of the linear and volume magnetostriction interaction can be of the same order of magnitude. However, the experiments that were carried out on Tb, Ho, and Dy showed an absence of critical attenuation for transverse waves [18, 49] (see Figs 1 and 2). These experimental results verified in Refs [59, 60] disagree with the above explanation. Later experiments showed that when the transverse waves propagate in the basal plane in Tb and Ho, they exhibit critical attenuation only if they have a certain polarization [61]. In order to explain these experimental results, the following mechanism was suggested in Ref. [60]. The rare-earth metals Tb, Dy, and Ho have a hexagonal structure and belong to easy-plane magnets. The energy of single-ion anisotropy stabilizes the spins in the basal plane and, consequently, the fluctuations along the c axis are suppressed by this energy, whereas the fluctuations in the basal plane are not restricted. The attenuation coefficient for the transverse waves is proportional to the correlation function for the spin components along both the propagation direction and the polarization vector. Therefore, no critical attenuation is observed for transverse waves of any polarization propagating along the c axis. The transverse waves only reveal anomalous attenuation if their polarization and propagation vectors lie in the basal plane.

Unlike the rare-earth and other metals, the attenuation coefficient in magnetic insulators exhibits less singular behavior. As in other magnetically ordered crystals, the total attenuation in magnetic insulators increases with increasing frequency. However, no anomalous attenuation is observed at high frequencies if the condition $\omega\tau > 1$ is fulfilled. In EuO, no anomalous attenuation was found near T_c in the frequency range 10–200 MHz [18]. A wide maximum of α_k was revealed below T_c; as measurements in a magnetic field of 8 kOe show, this maximum is due to the interaction of elastic waves with spins located in domain walls. A comparison of the interaction constants of EuO and other magnetic insulators shows that in the frequency range studied, EuO should exhibit anomalous attenuation of the same order of magnitude as that in MnF_2. The absence of critical attenuation in EuO can be explained by the anomalously large relaxation time, which satisfies the condition $\omega\tau \gg 1$; note also that it was mentioned in Ref. [62] that critical attenuation in europium oxide can be directly observed at frequencies of a few kilohertz.

In single crystals of ferrites with spinel (Fe_3O_4) and garnet ($Y_3Fe_5O_{12}$, $Gd_3Fe_5O_{12}$) structures, the anomalies in the velocity and attenuation of longitudinal waves were found to occur along all principal crystallographic directions. Both the velocity and attenuation reveal weak anisotropy; in particular, in yttrium iron garnet, it turns out to be

$$\frac{(\Delta v/v_0)_{[110]}}{(\Delta v/v_0)_{[100]}} = 1.28\,.$$

The anisotropy of α_k and Δv may be caused by the anisotropic dependence of the exchange integral on the interatomic spacing or by the contribution of the single-ion mechanism of spin–phonon interaction. This is also indicated by the data on thermal expansion of iron garnets [63].

It follows from the experimental data on ferrites with spinel and garnet structures that the attenuation grows in magnitude with increasing frequency and the maximum of α_k is displaced toward lower temperatures. In $Y_3Fe_5O_{12}$, the anomalous attenuation passes through a maximum at $T = T_{max}$ as the frequency increases from 1.67 to 30 MHz; the maximum attenuation is observed at 10 MHz [32, 33]. A similar phenomenon was revealed in yttrium iron garnet when measuring the complex susceptibility of the paraprocess at the same frequencies [64]. It is evident that the anomalous absorption of the elastic and electromagnetic energy in $Y_3Fe_5O_{12}$ may be related to the formation of domains with a strong correlation between spins, which have a finite volume and a most probable life time, according to our estimations, of about $\sim 10^{-8}$ s, which coincides with the data obtained from the measurements of dynamic susceptibility and neutron scattering [64, 65].

Unlike other rare-earth metals and metallic magnets, the critical behavior of gadolinium has not been determined unambiguously even in the hydrodynamic region. The dynamic critical properties of gadolinium were studied in Refs [18, 27–38], where it was shown that depending on the purity of a sample, gadolinium may be classified as either an isotropic or a uniaxial Heisenberg ferromagnet.

This information was obtained from experiments on the critical propagation of ultrasonic waves, since gadolinium is not an object that is suitable for using conventional methods of studying critical dynamics (neutron scattering, dynamic susceptibility, EPR). Note also that, although the experimental data available in the literature involve a wide range of temperatures and frequencies, they allow studying the dynamics of critical fluctuations only in the hydrodynamic region. To study the propagation of ultrasonic waves in the critical region, measurements in the immediate vicinity of T_c are necessary, which naturally increase the requirements on the experimental procedure. In particular, the accuracy of temperature maintenance and the temperature steps during the measurements should be no worse than 10^{-4} and 10^{-3} K, respectively. The critical region can also be achieved by increasing the frequency, but in this case the total attenuation increases sharply, which restricts measurements in the ordered phase to the condition $\omega\tau = 1$. In this connection, the optimal ranges for experimental investigation of the critical dynamics of gadolinium are frequencies of about 5–30 MHz and reduced temperatures $t \sim 10^{-4}-10^{-1}$.

Figure 5 displays typical temperature dependences of the total attenuation coefficient (at 25 MHz) and the relative change (at 10 MHz) in the velocity of longitudinal waves propagating along the c axis of gadolinium. Note that, like in other magnetically ordered crystals, the anomalies of α_k and $\Delta v/v_0$ do not coincide with $T_c = 293.575$ K, which was determined from magnetic measurements by the kink method, but are shifted toward lower temperatures. Moreover, the temperatures at which the maximum of α_k and the

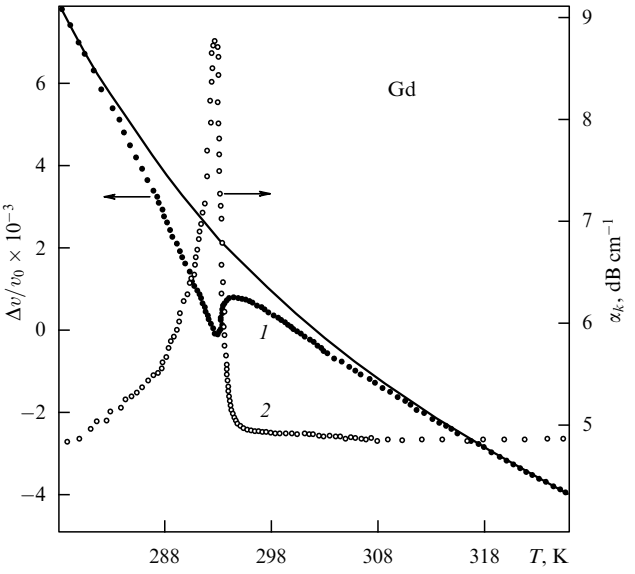

Figure 5. Temperature dependences of the velocity shifts (curve *1*, 10 MHz) and attenuation coefficient (curve *2*, 25 MHz) for gadolinium [83].

minimum of $\Delta v/v_0$ occur do not coincide with one another. Thus, at $\omega/2\pi = 10$ MHz the anomalies of α_k and $\Delta v/v_0$ are displaced with respect to T_c by 0.16 and 0.22 K, respectively. A characteristic feature of the frequency dependence of the attenuation is not only an increase in the α_k magnitude and a displacement of its maximum toward lower temperatures with increasing frequency, but also the absence of relaxation anomalies caused by trivial effects of the interaction of sound waves with domain walls.

To further discuss the experimental data and compare them with theory, one should determine the critical attenuation $\Delta\alpha_k = \alpha_k - \alpha_0$ (α_0 is the background attenuation) and the relative change in the sound velocity $(\Delta v/v)_k = \Delta v/v - \Delta v/v_0$ ($\Delta v/v_0$ is the normal change in the velocity).

In the paramagnetic phase, where the time average of the order parameter is zero, the only mechanism of anomalous attenuation is the fluctuation mechanism and it is assumed, when determining $\Delta\alpha_k$, that the background attenuation is independent of temperature. Since the anomalous attenuation is observed over a relatively narrow temperature range, the value of α_k is chosen as an α_0 value at a temperature that is 20–30 K above T_c. The normal change in the velocity is determined by the extrapolation of experimental values of $\Delta v/v_0$ measured in the paramagnetic phase to T_c.

Measurements of the velocity of both the longitudinal and transverse waves over a wide temperature range (78–900 K) performed in ferrites with spinel and garnet structures (see Refs [34, 35]) show that v in the paramagnetic phase decreases linearly with increasing temperature. Therefore, in order to find $(\Delta v/v_0)_k$, we used linear extrapolation. Taking into account that $\Delta v/v_0$ for gadolinium in the paramagnetic phase depends on T nonlinearly and that the ΔE effect in the ferromagnetic phase does not exceed 2%, for determining $(\Delta v/v_0)_k$ both at $T > T_c$ and at $T < T_c$, the following dependence was used:

$$\frac{\Delta v}{v_0} = a_0 + a_1 T + a_2 T^2 ,$$

where $a = 0.43524$, $a_1 = -2.6425 \times 10^{-3}$, and $a_2 = 3.977 \times 10^{-6}$. In Figure 5, this dependence is given by a solid line.

Experimental data show that when determining $\Delta\alpha_k$ and $(\Delta v/v)_k$ in a magnetically ordered phase, it should be remembered that the anomalous propagation of ultrasonic waves can be related not only to the second-order phase transformation, but also to the interaction of the sound with domain walls, spin waves, and nuclear spins. These interactions can lead to additional anomalies near the Curie point [55, 67]. Some of them are revealed in crystals that were studied in our work as well. An interaction with the domain walls, which led to a relaxation maximum, was revealed in ferrites of the copper–cadmium system. Near the Curie temperature, this maximum, unlike that caused by fluctuation effects, is suppressed even in a weak magnetic field. A resonance attenuation due to the interaction of elastic and spin waves was revealed in yttrium iron garnet [68]. At frequencies of 5–30 MHz, its maximum is observed relatively far from T_c and therefore it has no significant effect on the critical attenuation. Thus, for example, according to our data for $Y_3Fe_5O_{12}$ at $\omega/2\pi = 30$ MHz, the attenuation peak of the natural magnetoacoustic resonance is at $T = 530$ K, i.e., 20 K below T_c.

The temperature dependences of $\Delta\alpha_k$ and $(\Delta v/v)_k$ determined by the above methods correspond to the power laws

$$\frac{\Delta\alpha_k}{\omega^2} = B_0^{\pm} t^{-\eta_i^{\pm}} , \tag{3.1}$$

$$\left(\frac{\Delta v}{v}\right)_k = V_0^{\pm} t^{-n_i^{\pm}} , \tag{3.2}$$

where the plus and minus signs refer to the temperatures $T > T_c$ and $T < T_c$, respectively. The values of the critical exponents $(\eta_i^{\pm}, n_i^{\pm})$ and amplitudes $(B_0^{\pm}, V_0^{\pm})$ that best describe the experimental data are given in Tables 2–4.

When determining critical exponents and amplitudes, it should be remembered that their absolute values depend not only on the correct estimation of the background attenuation and the normal change in the velocity, but also on the choice of T_c. If T_c is identified with the attenuation-peak temperature or velocity minimum, then even for the same crystal the values of the critical exponents may vary within wide limits. For example, for gadolinium the values of η_i given by different authors vary from 1.2 [47] to 1.8 [69]. This may be due to the fact that, as we saw above, the anomalies in $\Delta\alpha_k$ and $\Delta v/v$ are observed below T_c and the anomalies themselves become displaced toward lower temperatures with increasing frequency.

To clarify the effect of the choice of T_c, we analyzed the dependences of η_i and n_i on T_c and found that a change in T_c of 1 K leads to changes in the critical exponents by 30% and more. Therefore, there is a need to determine T_c from independent measurements. The preference here should be given to estimating T_c from magnetic measurements using the kink method [66].

Moreover, the power laws (3.1) and (3.2) predicted by different theories are only valid if the condition $\omega\tau \ll 1$ is fulfilled. This means that the experiments and data treatment must be carried out in the corresponding frequency and temperature ranges. All these requirements are satisfied when the critical exponents given in Tables 2–4 are used. It follows from these tables that the n_i value is independent of the crystal structure, crystallographic direction, and of the range of exchange interaction and spin ordering. This can be shown using the data for single crystals of ferrites Fe_3O_4

Table 2. Experimental values of the critical exponents for the attenuation (η_i) and velocity (n_i) for magnetically ordered crystals.

Material	$t = (T - T_c)/T_c$	η_i	n_i	Ref.
Gd	$7 \times 10^{-3} - 7 \times 10^{-2}$	1.2 ± 0.1	0	[47]
	$10^{-3} - 10^{-1}$	1.63 ± 0.1	–	[18]
	$3.4 \times 10^{-3} - 2.4 \times 10^{-2}$	1.8 ± 0.2	–	[69]
Tb	$7 \times 10^{-3} - 7 \times 10^{-2}$	1.24 ± 0.1	0	[18]
Dy	$3 \times 10^{-3} - 10^{-1}$	1.37 ± 0.1	0	[18]
	–	1.26 ± 0.1	–	[18]
Ho	$3 \times 10^{-4} - 10^{-1}$	1.0 ± 0.1	0	[18]
	$2 \times 10^{-3} - 10^{-2}$	0.9 ± 0.2	0.25 ± 0.1	[59]
MnP	$5 \times 10^{-3} - 1.1 \times 10^{-2}$	1.1 ± 0.1	0.17	[31]
Ni	$3 \times 10^{-4} - 10^{-3}$	1.4 ± 0.2	–	[24]
	–	1.25	–	[25]
Rb_2CoF_4	$5 \times 10^{-3} - 2.5 \times 10^{-2}$	0.74 ± 0.05	–	[29]
EuO	–	0	$0(\ln t)$	[18]
$RbMnF_3$	$4 \times 10^{-4} - 4 \times 10^{-2}$	0.28 ± 0.05	0	[21]
	–	0.32 ± 0.02	–	[18]
MnF_2	$10^{-4} - 3 \times 10^{-2}$	$0.13 - 0.16$	0.12	[54]
	–	± 0.02	0.33	[18]
FeF_2	–	0.75 ± 0.08	–	[18]
Fe_3O_4	$2.3 \times 10^{-4} - 3 \times 10^{-2}$	–	0.25 ± 0.05	[42]
$Y_3Fe_5O_{12}$	$1.8 \times 10^{-4} - 3 \times 10^{-2}$	0.50 ± 0.10	0.32 ± 0.02	[42]
$Gd_3Fe_5O_{12}$	$2.3 \times 10^{-4} - 5 \times 10^{-1}$	0.42 ± 0.10	0.36 ± 0.05	[42]

Table 3. Critical exponents for the velocity (n_i), attenuation (η_i), and relaxation time (x) for some magnetic insulators.

Magnetic material	α	η_i	n_i	x^-	x^+	τ_0^-, 10^{-11} s	τ_0^+, 10^{-11} s	y^-
MnF_2	−0.11	0.14	0.12	0.83	0.15	50	106	−0.66
$RbMnF_3$	−0.14	0.28	0	0.48	0.21	1.12	7.43	−0.11
$Y_3Fe_5O_{12}$	−0.21	0.50	0.32	0.90	0.10	2.30	92.2	−0.50
$Gd_3Fe_5O_{12}$	−0.20	0.42	0.36	0.94	0.12	2.40	115	−0.53

(spinel structure), $Y_3Fe_5O_{12}$ (garnet structure), $Gd_3Fe_5O_{12}$ (garnet structure), and ferromagnetic metal gadolinium (hexagonal structure), as well as antiferromagnetic $RbMnF_3$ (cubic structure) and MnF_2 (tetragonal structure) and the weak ferromagnet NiF_2.

Thus, the insignificant changes in n_i when going from sample to sample and the closeness of n_i to the values of the critical exponent of the heat capacity (see Table 3) show that the propagation velocity of longitudinal waves gives information on the static critical behavior and, therefore, all the magnetic insulators that were studied can be classified based on the equalities $n_i = \alpha = a$ to the Heisenberg universality class ($d = 3$, $n = 3$).

The critical exponents for MnF_2 and $RbMnF_3$ given in Table 3 were borrowed from Refs [18, 55, 58], whereas the τ_0 and y^- values were calculated from experimental data given in those papers.

As to the critical exponent for the attenuation η_i, its values, as seen from Tables 2–4, are independent of the frequency and the propagation direction of longitudinal waves but depend on the range of the exchange interaction; for gadolinium, η_i is much greater than for ferrites with spinel and garnet structures. As can be seen from Table 1, this experimental fact agrees with the data obtained for other metallic and insulating magnetic crystals [18, 55–61].

Thus, from the experimental data on the velocities and attenuation of ultrasonic waves, the numerical values of the critical exponents for the attenuation, and the displacement of the maximum of α_k toward lower temperatures, it follows that in all the crystals that were studied both the fluctuation and relaxation mechanisms of anomalous sound propagation are observed. In the paramagnetic phase, only the fluctuation mechanism is present, which exhibits specific features in magnetic insulators and in metals.

Table 4. Critical exponents and amplitudes for gadolinium (along the c axis).

Critical exponents and amplitudes	$T > T_c$			$T < T_c$	
	Experiment	Theory		Experiment	Landau–Khalatnikov theory
		uniaxial ferromagnets	isotropic ferromagnets		
η_i	1.15(5)	1.218	1.883	1.08(5)	1.0
n_i	0.20(2)	−0.03	0.122	0.14(2)	0
x	0.92(7)	1.25	1.67	0.94(7)	1.0
y	0.08(4)	0.123	0.147	0.06(4)	0
z	1.37(10)	2.17	2.48 1.98	1.39(10)	2
B_0, $cm^{-1}\ s^2$	$5.0(1) \times 10^{-21}$		4.72×10^{-21}	$2.36(1) \times 10^{-19}$	
V_0, $10^4\ cm^3$	4.0(1)		4.16	9.5(1)	
τ_0, 10^{12} s	3.06		3.29	17.7	
B_F, $cm^{-1}\ s^{0.92}$	2.95×10^{-9}		—	—	
B_R, $cm^{-1}\ s^{0.94}$	—		—	1.29×10^{-8}	

4. Fluctuation mechanism of anomalous propagation of ultrasonic waves

4.1 Fluctuations of spin-energy density

In magnetically ordered crystals with strongly developed fluctuations, the dominating mechanism of the anomalous propagation of sound waves near the temperature of transformation into the paramagnetic state is the fluctuation mechanism, which consists in the following. Through the spin – phonon interaction of magnetostrictive nature, fluctuations of the order parameter or spin density produce a random force f_k, which disturbs the normal acoustic modes. As a result, an elastic wave propagating in such a system experiences decay and a frequency shift, which, according to Tani and Mori [17] and Kawasaki [8], are expressed through the correlation function of random forces. In particular, the attenuation coefficient is

$$\alpha_k = \mathrm{Re}\int_0^\infty \mathrm{d}t\,\big(f_k(t), f_k^*(0)\big)\,\frac{\exp(-\mathrm{i}\omega_k t)}{v_\mathrm{L}}\,(b_k, b_k^*)\,, \qquad (4.1)$$

and the change in the velocity of longitudinal waves $\Delta v = \Delta\omega_k/k$ caused by the frequency shift consists of two parts

$$\Delta\omega_k = (\Delta\omega_k)_1 + (\Delta\omega_k)_2\,, \qquad (4.2)$$

$$(\Delta\omega_k)_1 = -\frac{1}{2\rho k_\mathrm{B} T V \omega_k^0}\,\big\langle U_k^{(1)} U_{-k'}^{(1)}\big\rangle\,, \qquad (4.3)$$

$$(\Delta\omega_k)_2 = \frac{1}{\rho V \omega_k^0}\,\big\langle U_{kk'}^{(2)}\big\rangle\,, \qquad (4.4)$$

where $(\Delta\omega_k)_1$ is the second-order contribution from $\mathcal{H}_1$, and $(\Delta\omega_k)_2$ is the first-order contribution from $\mathcal{H}_2$. Unlike the case of α_k, the expression for Δv_k does not contain time correlations in the low-frequency limit. At high frequencies, (4.2) contains an additional term that determines the frequency dependence of the anomalous change in the velocity. It is only $(\Delta v_k)_1$ that exhibits singular behavior near T_c and, as both experimental [18, 24–26] and theoretical [43, 70, 71] studies as well as our data show (see Table 3), this part of the velocity change is proportional to the magnetic contribution to the heat capacity or thermal expansion coefficient. The second term in Eqn (4.2), as can be seen from Eqn (4.4), behaves near T_c in the same manner as the internal energy of the spin system.

When using Eqn (4.1) for explaining experimental data on α_k in magnetic insulators, including ferrites, it should be remembered that in the spin – phonon interaction that determines the dynamics of the random force f_k, the predominant part is that that is proportional to the Hamiltonian of the spin-energy density $\mathcal{H}_k$. In this case, as was shown by Kawasaki [20], we have

$$\alpha_k \sim \omega^2\,\mathrm{Re}\int_0^\infty \mathrm{d}t\,\big\langle \mathcal{H}_k(t)\mathcal{H}_k(0)\big\rangle\exp(-\mathrm{i}\omega_k t)\,, \qquad (4.5)$$

and, consequently, the sound waves predominantly interact with the spin-energy density fluctuations. If it is assumed that the changes in $\mathcal{H}_k$ with time and, consequently, the decay of the spin-energy density fluctuations occur by thermal diffusion of spins and by spin – lattice relaxation, then we have

$$\alpha_k \sim \frac{\omega^2 C_\mathrm{H}\tau}{1+\omega^2\tau^2}\,, \qquad (4.6)$$

$$\frac{1}{\tau} = \frac{1}{\tau_\mathrm{S}} + \frac{1}{\tau_\mathrm{SL}} = \frac{k^2\varkappa}{C_\mathrm{H}} + \frac{\gamma_0}{C_\mathrm{H}}\,. \qquad (4.7)$$

Here, τ_S and τ_SL are the times of spin diffusion and spin – lattice relaxation, respectively; $\varkappa$ is the spin thermal conductivity; γ_0 is a constant; and k is the wave number.

To determine the dominating mechanism of the decay of spin-energy density fluctuations in magnetic insulators, including ferrites, the relaxation time and its temperature dependence must be found. To this end, the following formula (universal for all the mechanisms) obtained from data on $\Delta\alpha_k$ and $(\Delta v/v)_k$ may be used [43]:

$$\tau = \frac{v}{\omega^2}\,\frac{\Delta\alpha_k}{(\Delta v/v)_k} = \tau_0 t^{-x}\,. \qquad (4.8)$$

Although this formula was derived on the assumption that $\omega\tau \ll 1$ and that τ is frequency-independent, it was shown experimentally that it can be used up to $\omega\tau \sim 1$ [43]. The values of the critical amplitudes τ_0 and exponents x that best describe the experimental data are given in Tables 3 and 4. It follows from these data that τ exhibits only a weak singularity. Moreover, in the paramagnetic phase of the ferrimagnets, the critical exponents α, x, and a are equal within the experimental error and coincide with the corresponding values for other magnetic insulators MnF_2 and $RbMnF_3$ [18, 21, 55, 56]. The proportionality of τ to the magnetic part of the heat capacity and thermal expansion coefficient indicates that in ferrimagnets the dominating mechanism of the decay of fluctuations is spin – lattice relaxation. At $\tau = \tau_\mathrm{SL}$ and $\omega\tau \ll 1$, it follows from Eqn (4.6) that $\eta_\mathrm{i} = 2\alpha$. This equality, as is seen from Table 3, is sufficiently well satisfied for the ferrites with garnet and spinel structures and the magnetic insulators MnF_2 and $RbMnF_3$.

Microscopic calculation of τ_SL was performed for the first time by Huber for the magnetic insulators MnF_2, $RbMnF_3$, and EuO [72]. Although the calculation was based on the Einstein model for the phonon system and the Gaussian approximation for the spin-correlation function, not only the proportionality of τ_SL to the magnetic part of the heat capacity was shown, but also a satisfactory agreement with experimental values was obtained. The calculated values of τ_SL turned out to be greater by a factor of four for $RbMnF_3$ and by a factor of thirty for MnF_2 as compared to the experimental values [72]. Based on more realistic approximations (Debye model for the phonon system and the Lowesey – Mesevi correlation function [73]), Itoh [73] obtained excellent agreement with experimental data not only for the temperature dependence, but also for the numerical values of τ_SL. Similar calculations were performed by us for some ferrites with spinel and garnet structures. In particular, the critical amplitudes τ_0 calculated in the Itoh approximation agree within 10 – 20% with the experimental values given in Table 3. The good agreement between experimental values of τ_SL and those calculated based on the Huber and Itoh approximations indicates the spin – lattice type of relaxation in ferrimagnets. In this case, C_H in Eqn (4.6) may be replaced by the relaxation time τ_SL. Then, Eqn (4.6) describing the frequency and temperature dependences of the attenuation coefficient takes

the form

$$\alpha_k(\omega, T) = \alpha_\infty \frac{\omega^2\tau^2}{1+\omega^2\tau^2}\,, \tag{4.9}$$

where α_∞ is a constant for the critical region. Equation (4.9) was experimentally verified using the Heisenberg antiferromagnet $RbMnF_3$ [55] and yttrium and gadolinium iron garnets [42]. This dependence is represented on a double logarithmic scale in Fig. 6. The experimental points correspond to various frequencies and the straight line, to the calculation in the Itoh approximation [73] with

$$\alpha_\infty = 8.69\,\frac{RT_c}{18Mv^2}\,\frac{A}{\tau_0}\,\frac{\partial \ln J}{\partial \ln a}\ \text{dB cm}^{-1}\,.$$

The fact that the measured values of α in a frequency range of 1.67 – 30 MHz and the temperature range $10^{-4}-10^{-2}$ K lie on the same straight line confirms the frequency independence of τ and the spin – lattice nature of relaxation.

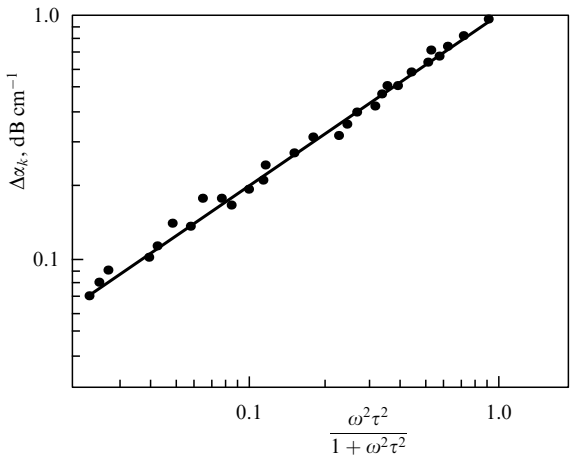

Figure 6. Critical attenuation in gadolinium and yttrium iron garnets as a function of $\omega^2\tau^2/(1+\omega^2\tau^2)$.

Thus, based on an analysis of experimental data on the velocity and attenuation of ultrasonic waves and a comparison of these data with theoretical concepts, we may conclude that in magnetic insulators, including ferrimagnets with spinel and garnet structures, the dominating factor in the paramagnetic phase is the linear interaction of sound waves with the spin Hamiltonian, and the anomalous attenuation is due to spin-energy density fluctuations, whose decay occurs through slow spin – lattice relaxation. The same mechanism can explain the absence of critical attenuation in EuO in the megahertz frequency range. According to Huber's calculations [72], $\tau_{SL} = 4\times10^{-6}$ s in EuO; then, $\omega\tau \gg 1$ in the frequency range of 10 – 200 MHz that was studied and, consequently, Eqn (4.9) yields $\alpha_k = \alpha_\infty$, which is nonsingular at the Curie point.

4.2 Fluctuations of the order parameter

It follows from the experimental data and the values of the critical exponents (see Tables 2 – 4) that in the paramagnetic phase in rare-earth metals, nickel, and MnP, the strength of the singularity of α_k is greater than in magnetic insulators. This is primarily due to the fact that in metallic magnets the exchange interaction is long-range. In magnetically ordered crystals of metallic type, there exist conduction electrons whose transitions from the s state into d or f states under the action of a random force, occuring near the Fermi surface, lead to local spin fluctuations. Therefore, the dynamics of the random force f_k is governed by long-wavelength spin fluctuations. In this case, if we neglect the contribution of $\mathcal{H}_2$, f_k is expressed through $U_k^{(\Gamma)}$ and the attenuation coefficient for longitudinal waves turns out to be proportional to the four-spin correlation function

$$\alpha_k = (2\rho V v_L)^{-1}\,\mathrm{Re}\sum_{q,q',\alpha,\alpha'} g_q^{\alpha^*}(k)\,g_{q'}^{\alpha'}(k) \times \int_0^\infty \left(S_q^\alpha(t)S_{-q-k}^\alpha(t), S_{-q'}^{\alpha'}(0)S_{q'+k}^{\alpha'}(0)\right)\exp(-i\omega_k t)\,dt\,,$$

$$g_q^\alpha(k) = \sum_j \exp(i\mathbf{q}\mathbf{R}_{ji})\left[\exp(i\mathbf{k}\mathbf{R}_{ji}) - 1\right]\mathbf{e}_k\,\frac{\partial J_{ij}^\alpha}{\partial \mathbf{R}_i}\,, \tag{4.10}$$

and the velocity change, as in the case of insulators, is described by Eqns (4.2) – (4.4).

The main difficulty in the theoretical discussion of critical propagation of sound waves consists in the estimation of the four-spin correlation function. Here, two approaches may be mentioned, namely, the so-called conditional theories [74 – 76] and the theories of Kawasaki [8, 22] and Laramore and Kadanoff [23]. The conditional theories, which are based on the representation of the four-spin correlation function through two-spin correlation functions by means of decoupling and on the use of the hydrodynamic form for estimating two-spin correlations, in the limit of $\omega\tau \ll 1$ yield $\alpha_k \sim \omega^2\chi^{1/2}\tau^{-1}$, i.e., lead to overestimated values of critical fluctuations. The Kawasaki theory [43], which is based on the concept of dynamical critical variables [8], and the Kadanoff's theory [23] of interacting modes yield identical values for the critical exponents. However, the latter theory makes it possible to estimate not only the critical exponents, but also critical amplitudes. Therefore, when comparing the experimental values of η_i, n_i, B_0, and V_0 with those calculated theoretically, predictions can be used that follow from the theory of interacting modes, according to which we have in the limit $\omega\tau \ll 1$

$$\Delta\alpha_k = B\omega^2\tau\,, \tag{4.11}$$

where

$$B = \frac{\rho k_B T_c \gamma v}{r_{c0}^3}\left(\frac{1}{T_c}\,\frac{\partial T_c}{\partial P}\right)^2 t^{2\alpha-2+3\nu}\,. \tag{4.12}$$

With this form of $\Delta\alpha_k$, it should be remembered that B is a singular quantity, whereas the experimentally determined amplitude B_0 is temperature-independent. For the first time, this circumstance was noted by Pokrovskii and Khalatnikov [77] when considering the anomalous sound attenuation near the λ point of helium. They showed that B had the same singularity as the heat capacity at constant pressure had. A similar result was also obtained for magnetically ordered crystals [70, 71]. However, V_0 cannot be estimated in terms of these works; we, therefore, theoretically calculated V_0 and n_i using the known formula for the relaxation time (4.8), which being combined with Eqns (4.11) and (4.12), yields

$$\left(\frac{\Delta v}{v}\right)_k = vB = V_0 t^{2\alpha-2+3\nu}\,. \tag{4.13}$$

Formulas (2.10), (2.11), and (4.11)–(4.13) also make it possible to obtain relations between the static and dynamic critical exponents:

$$\eta_i = x - 2\alpha + 2 - 3\nu = x - \alpha\,, \tag{4.14}$$

$$n_i = 2 - 2\alpha - 3\nu = -\alpha\,. \tag{4.15}$$

One of the main parameters that characterize critical dynamics is the relaxation time, which can be calculated from experimental data on $\Delta\alpha_k$ and $(\Delta v/v)_k$. In the paramagnetic phase, formula (4.8) is usually employed for this purpose, whereas in magnetically ordered phases, the $\tau(t)$ dependence can be restored from the displacement of the maximum of α_k with increasing frequency (according to the Landau–Khalatnikov relaxation theory, this displacement is determined by the condition $\omega\tau = 1$).

The temperature dependences of the relaxation time calculated from the data on $\Delta\alpha_k$ and $(\Delta v/v)_k$ show that the experimental points lie on two straight lines that represent power dependences of the type of (4.8) with identical critical exponents at both $T > T_c$ and $T < T_c$, but with different critical amplitudes (Fig. 7). Note that formula (4.8) is valid for gadolinium at $t \geqslant 10^{-3}$ ($\omega/2\pi = 30$ MHz, $\omega\tau = 0.39$), and the absolute values of τ coincide with the values given by other authors. Thus, Lüthi et al. [18] give $\tau = 5.31 \times 10^{-10}$ s at $t = 3 \times 10^{-3}$, whereas our data yield $\tau = 5.8 \times 10^{-10}$ s (see Fig. 7).

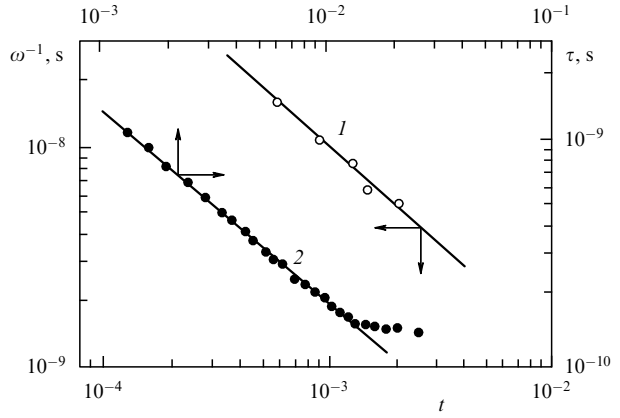

Figure 7. Temperature dependence of the relaxation time for gadolinium: *1*, at $T < T_c$; and *2*, at $T > T_c$ [83].

The final results obtained after mathematical treatment of the experimental data on the temperature and frequency dependences of α_k and $\Delta v_L/v_0$ that were performed by the least-squares method using a standard program are given in Table 4. The table also gives the numerical values of the critical amplitudes and exponents obtained in terms of the theory of interacting modes. When calculating critical amplitudes, the following values of the parameters that enter into expressions (4.11)–(4.13) were used: $v_L = 2.9 \times 10^5$ cm s^{-1}; $\rho = 7.9$ g cm^{-3}; $r_{c0} = a/\sqrt{6}$ (an estimation obtained from the molecular-field theory for hexagonal crystals; $a = 3.636$ A is the shortest spacing of atoms [23]); $dT_c/dP = 1.63 \times 10^{-3}$ K bar^{-1} [48]; and τ_0 was estimated, as in Ref. [23], on the assumption that the energy of critical fluctuations is equal to the exchange integral. The experimental and theoretical values of z given in Table 4, which are identical for various magnetically ordered crystals belonging to the same dynamic class of universality and are determined from the basic expression for the dynamic scaling [8–12]

$$\Omega_k = q^z f(qr_c)\,, \tag{4.16}$$

where Ω_k is the characteristic frequency of fluctuations with wave vector q, were calculated from the relationship $z = (\eta_i - n_i)/\nu$, which follows from Eqns (4.14) and (4.15), and from the well-known relation $z = x/\nu$ [12].

Note primarily that our values of the critical exponents η_i and n_i differ from those obtained by other authors: $\eta_i = 1.2 \pm 0.1$ [47], $\eta_i = 1.63 \pm 0.1$ [18], $\eta_i = 1.8 \pm 0.2$ [71], and $n_i = 0$ (logarithmic dependence) [18]. This difference appears to be related to the choice of the Curie point. In Refs [18, 47, 69], the Curie temperature was assumed to be equal to the temperature at which the attenuation peak was observed, whereas we determined T_c from magnetic measurements in weak magnetic fields (smaller than the anisotropy or demagnetizing fields [66]).

From a comparison of the experimental and theoretical critical exponents and amplitudes, three important results follow, which characterize the critical behavior of gadolinium in the hydrodynamic region. First, despite the significant discrepancies between the theory and experiment for some critical exponents, the critical propagation of ultrasonic waves can be described in terms of the theory of interacting modes by the isotropic Heisenberg model with a nonconserved order parameter (total spin of the system). In this case, the conservation of the total spin is disturbed by isotropic dipolar interactions (these problems are discussed below in more detail). Second, the critical amplitudes are less at $T < T_c$ than at $T > T_c$, which suggests the presence in the magnetically ordered phase of other than fluctuational mechanisms of anomalous variation of $\Delta\alpha_k$ and $\Delta v/v$, the most important of which is the Landau–Khalatnikov relaxation mechanism [7]. Third, the equality of the critical exponents $x^+ = x^-$ and $z^+ = z^-$ for gadolinium confirms the validity of the main assumption of the dynamic scaling hypothesis (4.17), according to which the characteristic frequencies of fluctuations are only a function of the variable $\omega\tau$.

5. Dynamic scaling for attenuation

It follows from the experimental and theoretical works [19, 27–31] that the total attenuation of ultrasonic waves in magnetically ordered crystals is caused by both the relaxation and fluctuations of the order parameter or spin-energy density. Below T_c, both mechanisms are operative, whereas in the paramagnetic phase, only the fluctuational mechanism is retained, i.e.,

$$\Delta\alpha_k^+ = \alpha_F^+\,, \qquad \Delta\alpha_k^- = \alpha_F^- + \alpha_R\,, \tag{5.1}$$

where α_F and α_R are the fluctuation and relaxation contributions to the critical attenuation $\Delta\alpha_k$.

According to the dynamic scaling concepts and the theory of interacting modes [19, 27–31], α_k is described in the entire critical region by the scaling function of the variable $\omega\tau$:

$$\alpha_k^\pm = B_F^\pm \omega^{1+y^\pm} f_F^\pm(\omega\tau^\pm)\,, \tag{5.2}$$

where $f(\omega\tau)$ is the scaling function. Its concrete form is not determined in the theory, but when treating experimental data, f_F is usually assumed to have the Lorentzian form

[27–31]

$$f_F^{\pm} = \frac{(\omega\tau^{\pm})^{1-y^{\pm}}}{C + (\omega\tau)^{1-y^{\pm}}} . \qquad (5.3)$$

Here, C is a positive constant, $y^+ = \alpha/x^+$, $B_F^+ = B_F^-$, and $\alpha_F^+ \neq \alpha_F^-$ because $\tau_0^+ \neq \tau_0^-$. Thus, we see that

$$\alpha_F^-(t) = \alpha_F^+(qt) , \qquad q = \left(\frac{\tau_0^-}{\tau_0^+}\right)^{1/x} . \qquad (5.4)$$

Then, using (5.2), we can determine α_F and α_R for the magnetically ordered phase. It was shown that not only α_F, but also α_R was described by the scaling equation [19]

$$\alpha_R(t) = \Delta\alpha^-(t) - \alpha_F^+(qt) = B_R\omega^{1+y^-} f(\omega\tau^-) , \qquad (5.5)$$

$$f(\omega\tau) = \frac{\omega\tau^-}{1 + (\omega\tau^-)^2} . \qquad (5.6)$$

A similar result follows from the Landau–Khalatnikov theory at $y^- = 0$ [7].

In order to experimentally verify scaling equations (5.2) and (5.5), we must determine y^-, y^+, and C. To this end, we may use the limits of the functions f_F and f_R at $T = T_c$ and $T = T_{max}$. Since $\omega\tau \to \infty$ at $T = T_c$ and $\omega\tau = 1$ at $T = T_{max}$, we have

$$\alpha_F^+ = B_F\omega^{1+y^+} = \alpha_c , \qquad T = T_c , \qquad (5.7)$$

$$\alpha_R = \frac{1}{2} B_R\omega^{1+y^-} = \alpha_{max} , \qquad T = T_{max} . \qquad (5.8)$$

Figure 8 displays the frequency dependence of α_k for gadolinium at these temperatures; it is seen that the experimental points satisfy dependences (5.7) and (5.8) in the frequency range 5–30 MHz. The value of $\Delta\alpha_k$ corresponding to 5 MHz was borrowed from Ref. [69].

The constant C is estimated from the experimental values of $\Delta\alpha_k$ at $T = T_c$ and $\omega\tau^+ = 1$. From Eqn (5.7) and the temperature dependence of $\Delta\alpha_k$, we have $\alpha_F^+/\alpha_c = 1/(C+1) = 0.75$ and $C = 0.33$.

The experimental data for α_F^+ in the frequency range 10–30 MHz were treated by the least-squares method using the above estimates for y^+ and C. As the adjustable parameters, we used x^+, y^+, and C, whose values were selected to be close to 0.9, −0.08, and 0.33, respectively. The best agreement of the experimental points with Eqn (5.2), which is shown by a dashed line in Fig. 9, was obtained at $x^+ = 0.91$, $y^+ = -0.12$, and $C = 0.30$. These data are in satisfactory agreement with the values that were obtained based on direct measurements (see Fig. 8 and Table 4).

The relaxation contribution α_R to the anomalous attenuation was found using Eqns (5.4) and (5.5) with $q = 6.8$. The scaling function for α_R on the double logarithmic scale is also shown in Fig. 9 (curve *2*). Here, the data points of various forms correspond to different frequencies and the dashed line represents Eqn (5.5) with $y^- = 0.12$. The numerical values of the other parameters necessary for the calculations are given in Table 4. As can be seen from Fig. 9, the experimental data on the frequency and temperature dependences of α_k in the range of $\omega\tau$ from 0.1 to 7.0 relatively well satisfy Eqn (5.5). The maximum of α_R occurs not at $\omega\tau = 1$, as expected from the Landau–Khalatnikov theory, but somewhat displaced

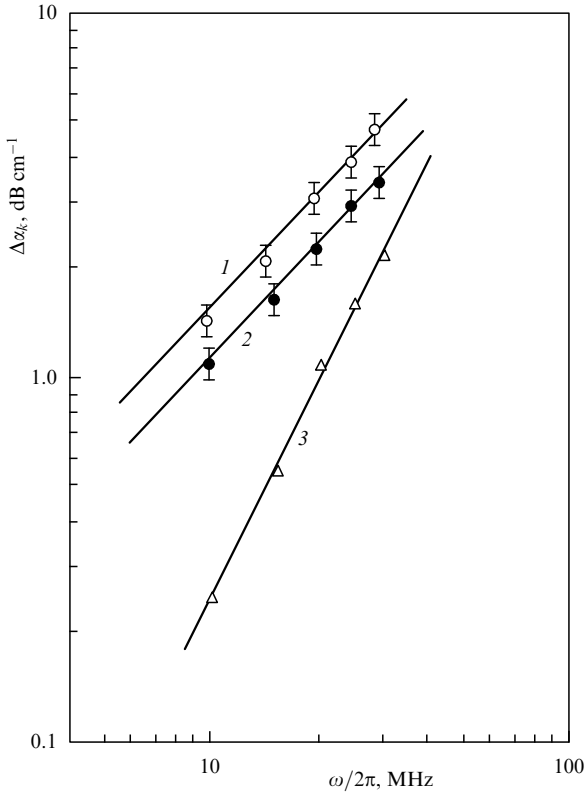

Figure 8. Frequency dependence of critical attenuation in gadolinium at various temperatures: *1*, $T = T_{max}$; *2*, $T = T_c$, and *3*, $t = 10^{-3}$ [83].

toward the greater values of $\omega\tau$. This displacement ($\omega\tau = 1 - y^- = 1.12$), caused by the singularity of the critical amplitude of the attenuation coefficient, leads in turn to a displacement of the maximum of $\Delta\alpha_k$ and the minimum of $\Delta v/v$ relative to one another.

Similar behavior of the ultrasonic attenuation is also observed in other metallic magnetic materials. In particular, in the ferromagnetic compound MnP, whose static critical behavior is described by the three-dimensional Ising model ($\beta = 0.34 \pm 0.03$ and $\gamma = 1.29 \pm 0.05$), the investigation of the critical propagation of ultrasonic waves (30–210 MHz) along the hard axis (*a* axis) showed that in the range $0.1 < \omega\tau < 10$, the attenuation is described by the scaling function (5.2) [31]. In this case, $x^+ = x^- = 0.92 \pm 0.05$, $\tau_0^+ = 9.0 \pm 0.15$, $q = 5.0 \pm 0.5$ and $y^+ = y^- = -0.18 \pm 0.04$ [31]. The fluctuation contribution found from the total attenuation both above and below T_c is described by Eqns (5.2) and (5.3) with $C = 2.0 \pm 0.2$. The behavior of the relaxation contribution is asymmetric relative to $\omega\tau^- = 1$, although it is described by the scaling function (5.5). Figure 10 displays (on a double logarithmic scale) the relaxation contribution as a function of $\omega\tau^-$. At small $\omega\tau^-$, the experimental points correspond better to the Lorentzian function (5.6), whereas at $\omega\tau^- > 1$, a Gaussian function yields a better approximation.

The dynamic exponent for MnP ($z = 1.38$) estimated from the relation $z = x/v$ proved to be much less than the theoretical value $z = 2$ for a three-dimensional Heisenberg ferromagnet with nonconserved order parameter [12]. In accordance with the assumption of the possibility of describing the phase transition in MnP on the basis of the molecular-field theory [27], the value $v = 1/2$ was used when estimating z, which yields $z = 1.84 \pm 0.10$. This result is close to the value

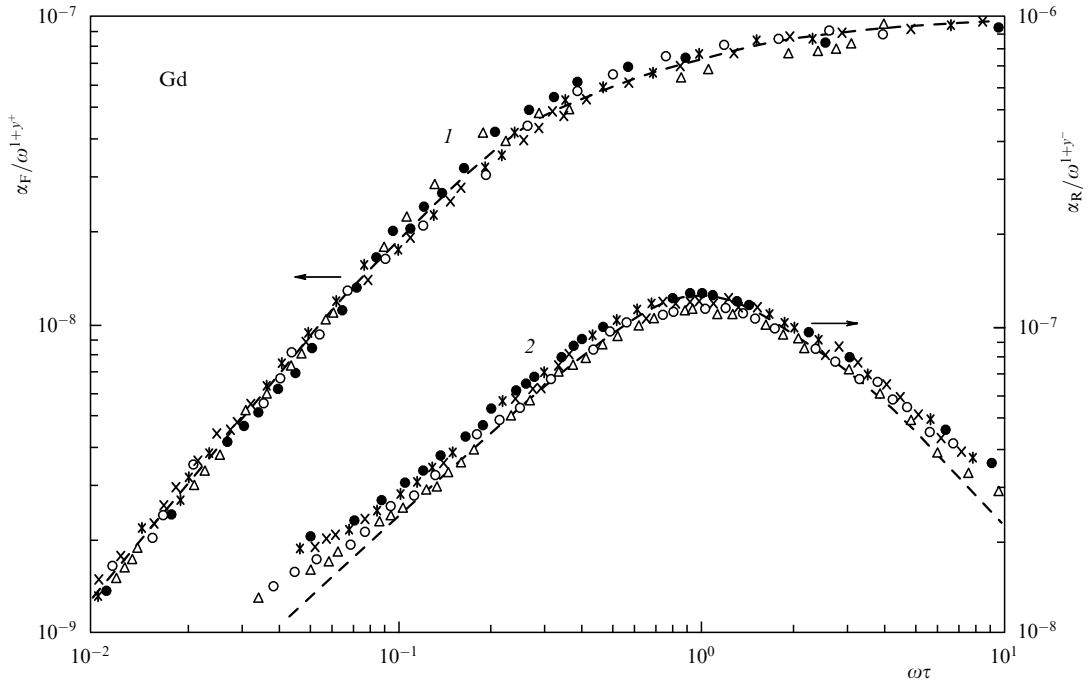

Figure 9. Scaling equations for the fluctuation (curve *1*, $T > T_c$) and relaxation (curve *2*, $T < T_c$) contributions to the anomalous attenuation in gadolinium [83].

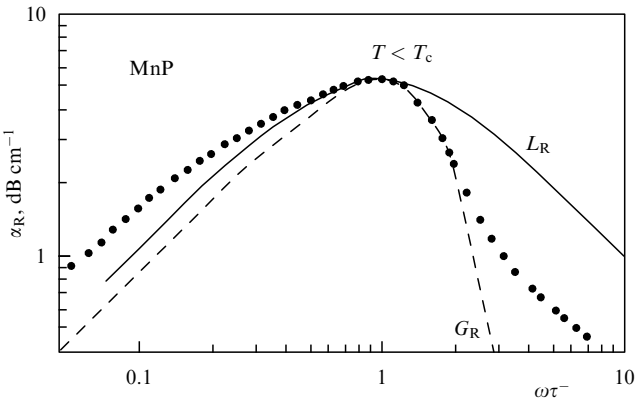

Figure 10. Scaling equation for the relaxation contribution in MnP [31]. L_R and G_R are the Larmor and Gaussian functions, respectively.

that follows from the Landau – Khalatnikov [7] and Van Hove [8] theories.

A disagreement between the static critical behavior and the dynamic behavior was also revealed in the two-dimensional Ising antiferromagnetic compound Rb_2CoF_4 [30]. Ultrasonic studies performed in the frequency range of 10 – 150 MHz yield $x^+ = 1.20 \pm 0.10$ and $x^- = 1.23 \pm 0.05$. It follows from these values that at $\nu = 0.99 \pm 0.04$, we have $z = 1.21 \pm 0.10$. This result agrees with the predictions of dynamic scaling for the two-dimensional isotropic antiferromagnet ($z = d/2$), but disagrees with the values obtained by the Monte Carlo and the renormalization-group methods for the kinetic Ising model ($z = 1.85 - 2.18$) [30].

As to the ferrimagnets, the main contribution to the anomalous attenuation at $T < T_c$ comes from the relaxation mechanism because of the weak singularity (caused by the interaction of the sound waves with fluctuations of the spin-energy density) of the attenuation coefficient. The critical exponents and amplitudes that characterize the behavior of this contribution are given in Table 3. Note that the critical exponents and the relaxation-time amplitudes differ from their values in the paramagnetic phase. A similar phenomenon was also revealed in other magnetic insulators [55, 57]. In particular, the values of x^- for the ferrimagnets are close to those predicted by the Landau – Khalatnikov theory, and the critical amplitudes of the relaxation time are less by an order of magnitude or even more than those characteristic of the paramagnetic phase. In addition, the frequency dependence of α_R at $T = T_{max}$ in yttrium and gadolinium iron garnets is described by the values of $y^- = -0.50 \pm 0.05$ and $y^- = -0.53 \pm 0.05$, respectively, which are much greater than those in metallic magnets. The numerical values of y^- for magnetic insulators (see Table 3), including ferrites, may be theoretically justified on the basis of Suzuki's concepts [28], according to which we have in the magnetically ordered phase

$$\alpha_R \sim \omega M^2 \chi(q) f_R(\omega\tau^-)\,, \tag{5.9}$$

where M is the magnetization, and $\chi(q)$ is the dynamic susceptibility. For $qr_c \to 0$, $\chi(q) \sim t^{-\gamma}$, and $M \sim t^{-\beta}$, it follows from Eqn (5.9) that $y^- = (2\beta - \gamma)/x^-$. Substituting the values of the critical exponents β, γ^-, and x^- of MnF_2, $Y_3Fe_5O_{12}$, and $Gd_3Fe_5O_{12}$ into this relation, we obtain y^- values close to those of experiment (see Table 3).

Thus, in the magnetically ordered phase, the contribution to the anomalous attenuation in magnetic insulators, as in metallic magnets, is described in terms of the dynamic-scaling concept.

5.1 The concept of dynamic scaling

The main parameters that determine the critical dynamics are the critical exponent of the relaxation time and the dynamic critical exponent z. Determining z is a complex problem; therefore, we shall dwell on it in more detail.

How dynamical exponents determined by statics can arise may be illustrated by an analysis of dynamic critical phenomena in a $4-\varepsilon$-dimensional space [2].However, many questions remain unanswered. Seemingly, the Hamiltonian contains the entire information on the dynamics of a system. Nevertheless, to date no one has been able to obtain the equations of the dynamical renormalized group starting from the microscopic Hamiltonian. Thus, the question of the construction of a dynamic theory starting from the microscopic Hamiltonian still remains open.

Nevertheless, many studies of dynamical phenomena are based on microscopic Hamiltonians of the spin system. For these models, calculations of z were performed on the basis of the theory of interacting modes [3, 23], dynamic scaling [3, 4], and the renormalized-group theory [4, 6]. The theoretical difficulties are, of course, incomparable with the experimental ones; but the first consideration is that experiments do not ensure the accuracy that is necessary for the theory.

Despite the above remark, it is worth considering some thorough experimental investigations on neutron scattering, particularly in ferromagnets with high Curie temperatures (Ni, Fe, etc.). All the z values obtained by this method are very close to that of the Heisenberg ferromagnet (cf. the results of Tables 5 and 6). Similar results were obtained using the methods of neutron spin echo [95], perturbed angular correlations [94], and Mössbauer spectroscopy. However, even in the case of nickel, which was studied in most detail by both neutron scattering and ultrasonic methods, the z values differ so much from one another that it is impossible to make definite conclusions on the character of the dynamic fluctuations. Note, nevertheless, that the z values obtained for Ni make it possible to classify this material as a Heisenberg ferromagnet.

Even more complex is the situation in the case of the rare-earth metal gadolinium, which, according to all data, is a Heisenberg ferromagnet [82, 83]. Gadolinium was investigated using both ultrasonic methods [18, 47, 83], Mössbauer spectroscopy [79] and the disturbed angular correlation method [81, 82]. The range of z obtained is so wide that it includes both the value characteristic of rigid dipolar dynamics ($z=1$) and the value specific of a Heisenberg ferromagnet ($z=2.5$). Note also that in magnetic insulators, the determination of z is impossible because of the specific features of spin–lattice relaxation in them.

The above brief analysis by no means implies that it is impossible to correctly determine the dynamic critical exponent z using the above methods. It is likely that this can be made with a correct choice of the object of study and appropriate ranges of frequency, temperature, and magnetic fields and, which is the most important, the correct treatment and interpretation of the results obtained.

Table 5. Theoretically predicted values of the dynamical exponent z.

Spin-system model	Universality class of the static critical behavior	Scaling law	Approximate numerical values for $d=3$
Isotropic ferromagnet	$(3,d)$	$1/2(d+2-\eta)$	5/2
Isotropic antiferromagnet	$(3,d)$	$d/2$	3/2
Anisotropic ferromagnet	$(1,d)$	$2-\alpha/\nu$	2
Anisotropic antiferromagnet	$(1,d)$	$2-\alpha/\nu$	2
Ferromagnet with nonconserved order parameter	(n,d)	$2+c\eta$ $c=-0.5$	2
Ferromagnet with dipolar interactions:	$(3,d)$		
normal dynamics		$2-\eta$	2
		$2+c\eta$	
		$c=0.94$	2
rigid dynamics		$(5-\eta)/2-1/\nu$	1

Table 6. Experimental values of the dynamic critical exponent z.

Magnetic material	z	Measurement method	Remarks
Ni	2.46(25) [94]	NS	Crossover to the dynamics of
	2.5 2.0 [95]	PAC	systems with nonconserved
	2.5 2.0 [96]	MS	spin at $t<3.9\times10^{-3}$
	2.0 (0.3) [24]	US	Hydrodynamic
	1.78 [25]	US	region
Gd	1.36–1.52 [79]	MS	Crossover to anisotropic behavior at $t<2\times10^{-3}$
	1.786(6) [81]	PAC	
	1.73(5) [82]	PAC	
	1.37(10)–1.80(10) [83]	US	Crossover to dipole dynamics at $t<2.6\times10^{-2}$
	1.7(2) [47]	US	Hydrodynamic region
	2.3(2) [18]	US	
	2.6(2) [69]	US	
MnP	1.38(10) [31]	US	Dynamics are assumed to be
	1.37(6) [27]	US	close to classical ($z=2$)
$RbMnF_3$	1.4(2) [97]	LS	
MnF_2	1.5(2) [97]	LS	Crossover from isotropic to anisotropic behavior at $t<3.5\times10^{-2}$
	1.26	US	$T<T_c$
$Y_3Fe_5O_{12}$	1.35(10) [42]	US	$T<T_c$
Rb_2CoF_4	1.15(5) [98]	NMR	Two-dimensional Ising antiferromagnet
	1.21(10) [29]	US	

NS — neutron scattering,
PAC — perturbed angular correlation,
MS — Mössbauer spectroscopy,
US — ultrasonic methods,
NMR — nuclear magnetic resonance.

6. Effect of dipole forces on critical dynamics

Let us consider the effect of dipole forces on the critical dynamics of magnetically ordered crystals using gadolinium as an example. It is seen from Table 4 that the experimental critical exponents differ significantly from the theoretical values for the Ising ($n=1$) and Heisenberg ($n=3$) models. In particular, the critical exponent η_i is much less than the value that follows from Eqn (4.14) for the systems with $n=3$ but is close to the value for the systems with $n=1$. At the same time, the exponent n_i corresponds better to the Heisenberg model in both the sign and the absolute value. As to the critical exponents x and z, they are far from the values predicted by the theory for model crystals. This is true even for ferromagnets with nonconserved spin, although in this case the agreement between the theory and experiment is somewhat better (see the second line for z in Table 4). In gadolinium, the conservation of the total spin may be disturbed because of the presence of anisotropic and dipolar interactions.

The effects of the anisotropic and dipole – dipole forces on the static critical behavior of gadolinium were estimated in Refs [6, 80] to show that the crossover to dipolar behavior can occur starting from $t = 2.62 \times 10^{-2}$. In this connection, when analyzing experimental data on the critical propagation of ultrasonic waves in Gd, one should take into account the effect of dipolar forces. However, this question has not yet been clarified theoretically; therefore, we will use the general theory of the effect of dipolar forces on the critical dynamics of ferromagnets, which was considered in the reviews by Maleev [13 – 15]. According to his theory, ferromagnets can have both normal and anomalous (rigid) dipolar dynamics. The first is characterized by the critical exponents $x = (2 - \eta)\nu$ and $z = 2 - \eta$. The calculations performed by Teitel'baum [16] using an ε expansion yield a close value $z = 2 + 0.94\eta$. The rigid dipolar dynamics caused by the interaction of longitudinal and transverse (with respect to the momentum) fluctuations leads to $z = (5 - \eta)/2 - 1/\nu$ and $x = \left[(5 - \eta)/2 - 1/\nu\right]\nu$. By using the values of η and ν obtained by the ε expansion [2, 4, 6], we obtain $z = 1.977$ and $x = 1.368$ for the normal dynamics, whereas $z = 1.043$ and $x = 0.722$ for the rigid dynamics. The experimental values of z and x lie between these values, i.e., preference cannot be given to either of these dynamics. However, it is known that in ferromagnets the region of rigid dynamics narrows with increasing S and in gadolinium ($S = 7/2$) the occurrence of normal dynamics seems more realistic. Nevertheless, large discrepancies between the theoretical and experimental values of z and x remain; in our opinion, they can be explained by the following circumstances.

First, in the exchange region, the dipolar forces lead to the so-called Huber attenuation (see Ref. [13]), which is characterized by a decreasing relaxation time at $T \to T_c$: $\tau \sim t$. In gadolinium, we already have $4\pi\chi = 1$ at $t = 2.62 \times 10^{-2}$; therefore, the effect of the Huber attenuation on the temperature dependence of $\Delta\alpha_k$ should be insignificant. Nevertheless, it can lead to a decrease in the critical exponent η_i and, consequently, x and z. Second, almost the entire temperature range that was investigated for gadolinium corresponds to the region of crossover and therefore, by analogy with the static critical exponents, the experiment yields effective rather than asymptotic values of x and z [6]. For example, the critical exponent for the static susceptibility γ (through which η_i can be expressed as follows: $\eta_i = \gamma - \alpha$ for normal dynamics and $\eta_i = \gamma(5 - \eta)/2(2 - \eta) - 1 - \alpha$ for rigid dynamics) is 10% (or even more) less than the asymptotic value [6, 78]. This circumstance cannot be ignored when discussing experimental results. We should also remember that the above considerations are of a qualitative nature because of the absence of theoretical works devoted to problems of critical propagation of ultrasonic waves in the crossover region.

The agreement between the theoretical and experimental values can be improved by calculating z on the basis of the data on attenuation and the dynamic-scaling concept for $\Delta\alpha_k$ in the form [19]

$$\Delta\alpha_k(\omega) = r_c^{2/\nu - 3}\omega f(r_c^z\omega)\,, \tag{6.1}$$

from which the relation $\eta_i = (z - 3)\nu + 2$ follows for the hydrodynamic region ($r_c^z\omega \ll 1$). Calculations based on this relation yield $z = 1.80$. A close result is also obtained from Eqns (4.14) and (4.15) if, by analogy with the critical exponent α for the heat capacity, n_i is assumed to be negative for Heisenberg magnets (the more so because the critical change in the velocity at $T = T_c$ remains finite).

Note, finally, that the significant effect of dipolar forces on the critical dynamics of gadolinium is also indicated by studies performed by other methods [79 – 82]. The critical dynamics of gadolinium were studied by the electron paramagnetic resonance method at a frequency of 9 GHz [80]; the resonance linewidth in the paramagnetic phase was shown to have a maximum characteristic of only dipolar magnets [13 – 15, 82]. Moreover, the $\Delta H T\chi_\perp = f(\chi_\parallel)$ dependence, where $\chi_\parallel$ and $\chi_\perp$ are the longitudinal and transverse (with respect to the field) static susceptibilities and ΔH is the EPR linewidth, obeys a power law with an exponent 0.84, whereas for the Huber attenuation this exponent is equal to 7/4. The investigation of the critical dynamics of gadolinium by the $\gamma - \gamma$ perturbed angular correlation method shows that the fluctuations are isotropic, at least at $t > 3 \times 10^{-3}$, and the dynamic exponent z determined from the autocorrelation time assumes the values 1.3 – 1.52 [79], 1.786 [81], or 1.73 [82], which are in rather good agreement with our data [83] and the theoretical values for the normal dipolar dynamics [16].

Based on an analysis of experimental data for the propagation velocity and the attenuation of ultrasonic waves, it was shown above that in the magnetically ordered crystals studied all three mechanisms of interaction of ultrasonic waves with the internal degrees of freedom of the spin system manifest themselves. It was established that the dominating interaction mechanism depends on the exchange interaction range and the temperature region. In particular, in the paramagnetic phase, the dominant interaction is the linear coupling with the spin Hamiltonian in insulating magnets, and the quadratic coupling with fluctuations of the order parameter in metallic magnets. In the magnetically ordered phase, a linear coupling with the order parameter is added, which leads to relaxation attenuation of ultrasonic waves.

7. Effect of a magnetic field on the propagation of ultrasonic waves in the critical region

7.1 Paramagnetic phase

For the first time, the effects of a magnetic field on the propagation of sound waves near the Curie point in ferromagnets were considered by Belov, Kataev, and Levitin [84], who showed, based on the Landau – Khalatnikov theory [7], that Young's modulus decreases in a magnetic field and the attenuation maximum is shifted toward higher temperatures with increasing H. These results were later confirmed in their experimental studies of invar-type alloys.

In further investigations, it was established both experimentally and theoretically that the effect of a magnetic field on the propagation of ultrasonic waves is primarily determined by the character of the exchange interaction [85].

When studying the propagation of ultrasonic waves in rare-earth metals near the critical temperature in a magnetic field, some features were revealed that are caused by the long-range character of the s – f interaction [61, 69, 86]. In particular, in the paramagnetic phase, the magnetic field causes, on the one hand, a decrease in the attenuation coefficient α_k due to the suppression of spin fluctuations, and on the other hand, an increase, which is observed at a sufficient distance from T_c or near T_c in weak magnetic fields. The growth of α_k in weak magnetic fields is caused by the polarization of the spin system of localized 4f electrons, which

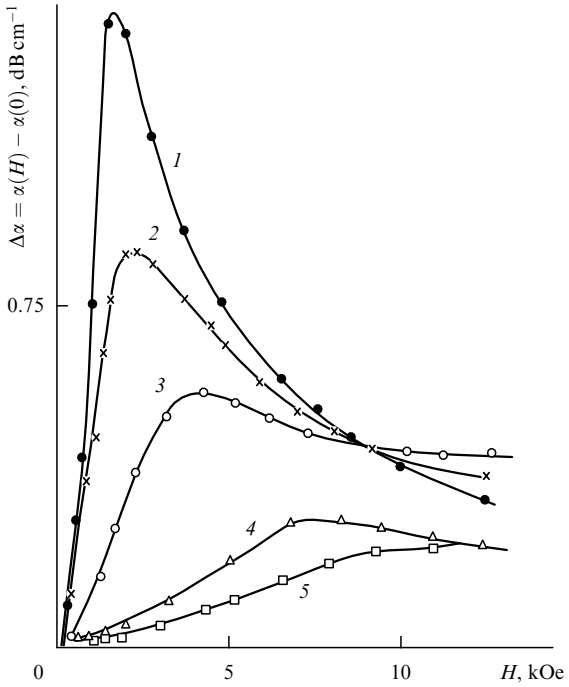

Figure 11. Variation of $\Delta\alpha$ as a function of H for gadolinium at various temperatures [91]: *1*, 294.21; *2*, 295.54; *3*, 297.12; *4*, 305.46; and *5*, 310.61 K; $H \parallel k$.

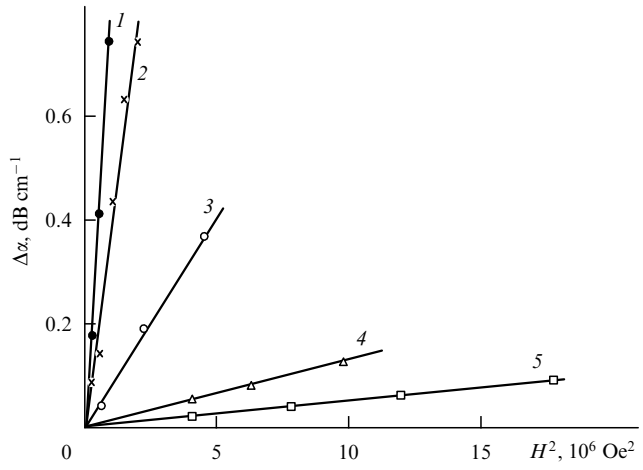

Figure 12. Variation of $\Delta\alpha$ as a function of H^2 for gadolinium [91]. For designations, see Fig. 11.

leads, through the s–f exchange interaction, to a shift of the energy-spin subbands of s electrons and, consequently, to additional acoustic losses [85–91]. This polarization mechanism of the anomalous change in α_k in a magnetic field was experimentally observed and theoretically justified for Ho, Tb, and MnP [51, 86, 90] and for Gd [66, 89, 91]. Let us consider the characteristic features of the influence of a magnetic field on the propagation of ultrasound near the critical temperature using gadolinium — a rare-earth metal with the simple ferromagnetic order in a hexagonal lattice.

The typical isotherms of the field dependences $\Delta\alpha = \alpha_k(H) - \alpha_k(0)$ and $\Delta v(H)/v(0) = [v(H) - v(0)]/v(0)$ for the paramagnetic phase of Gd given in Figs 11–14 show that in weak magnetic fields, $\Delta\alpha$ increases and $\Delta v(H)/v(0)$ decreases with increasing H. At not too weak fields, $\Delta\alpha$ and $\Delta v(H)/v(0)$

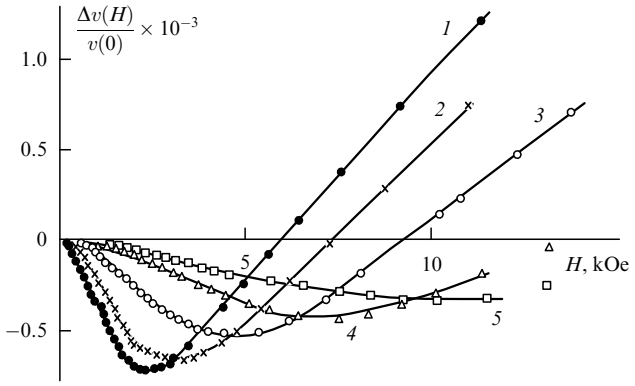

Figure 13. Variation of $\Delta v/v$ as a function of H for gadolinium at various temperatures [89]: *1*, 294.21; *2*, 295.54; *3*, 297.12; *4*, 305.46; and *5*, 310.61 K; $H \perp c \parallel k$.

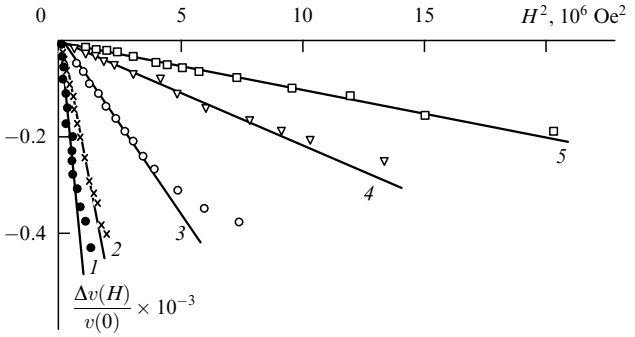

Figure 14. Variation of $\Delta v/v$ as a function of H^2 for gadolinium at various temperatures [89]. For designations, see Fig. 13.

pass through maxima, which shift with increasing T toward the greater fields. In strong fields, $\Delta\alpha$ and $\Delta v(H)/v(0)$ decrease and, starting from a certain field whose value depends on T, the velocity shift in the field becomes positive. Far from T_c, where spin fluctuations are weak, $\Delta\alpha$ and $\Delta v(H)/v(0)$ increase with increasing field. A similar picture is observed in all cases where the direction of the field and the direction of propagation of ultrasonic waves are mutually perpendicular.

As was shown by Tachiki and Maekawa [85], the effects of a magnetic field on the propagation of ultrasonic waves in metallic magnets are caused by the competition of the polarization and relaxation mechanisms:

$$\alpha_k = (2\rho V v_L)^{-1} \operatorname{Re}\Bigg[4g_0^{z*}(k)g_0^z(k)\langle S_0^z\rangle^2 \times \int_0^\infty \big(S_{-k}^z(t), S_k^z(0)\big)\exp(-i\omega_k t)\,dt + \sum_{qq'\alpha\alpha'} g_q^{\alpha*}(k)g_{q'}^{\alpha'}(k)\int_0^\infty \big(S_q^\alpha(t)S_{-q-k}(t), S_{-q'}^\alpha(0)S_{q'+k}^\alpha(0)\big) \times \exp(-i\omega_k t)\,dt\Bigg], \quad (H \parallel z), \tag{7.1}$$

where S_0^z is the spin polarization along the z axis. Here, the first term in square brackets is a result of the combined action of the polarization and fluctuation mechanisms and the second term represents fluctuations. In weak magnetic fields and if the spin polarization (magnetization) is proportional to H, it follows from (7.1) that $\alpha_k \sim H^2$.

For the paramagnetic phase of hexagonal crystals, the contributions to $\Delta\alpha$ and $\Delta v(H)/v(0)$ caused by the polarization mechanism are determined by the expressions [86]

$$\Delta\alpha = B\,\frac{H^2}{(T-\Theta)^3}\,\frac{\omega^2\tau}{1+\omega^2\tau^2}\,,$$
$$\frac{\Delta v(H)}{v(0)} = -Bv\,\frac{H^2}{(T-\Theta)^3}\,, \qquad (7.2)$$

where B is a constant that characterizes the magnetoelastic interaction and Θ is the paramagnetic Curie point, which is equal to the Curie temperature in the molecular-field approximation. Note that formulas (7.2) can be obtained from the theory of Tachiki and Maekawa [85] if the purely fluctuational term [second term in brackets in Eqn (7.1)] is neglected. The experimental studies of Gd (see Figs 12 and 14), Dy, Ho, and Tb [86, 90] show that in the paramagnetic phase of these metals, $\Delta\alpha$ and $\Delta v(H)/v(0)$ depend quadratically on the field H. As $T \to T_c$, fluctuations begin to play a progressively more important role; nevertheless, the experimental isotherms contain a region of magnetic field where the quadratic dependence predicted by formulas (7.2) remains valid. In accordance with Eqns (7.2), the slope of this dependence increases on approaching T_c.

If the condition $\omega\tau \ll 1$ is fulfilled, it follows from Eqns (7.2) that the relaxation time is independent of the temperature and magnetic field. Calculations of τ from the experimental data using formula (4.8) where $\Delta\alpha_k$ and $(\Delta v/v)_k$ are replaced by $\Delta\alpha$ and $\Delta v(H)/v(0)$ show that the relaxation time is independent of H for all the isotherms in the magnetic field region where the quadratic dependence is valid and the temperature dependence is sufficiently strong [86]. As follows from experimental data, the temperature dependence of T is described by a power law of the type of (4.8). The best agreement of the data points with this dependence is observed in the range $6.8\times10^{-3} \leqslant t \leqslant 5.82\times10^{-2}$ at $x^+ = 0.96(5)$. Thus, the character of the temperature dependence of the relaxation time in the magnetic-field range where the polarization mechanism dominates undergoes no significant changes in comparison with the case of $H = 0$ (see Table 4).

To quantitatively compare the experimental data with theory, changes in α_k and v_L were calculated using the formulas obtained by Tachiki and Maekawa [85]. For hexagonal crystals, the formulas have the following form:

$$\alpha_k^a = F_k t\left\{\left[\frac{M(1-b)}{t-(1-k_1)(1-b)}\right]^2 + Gt\left[\frac{1-b}{t-(1-k_1)(1-b)}\right]^{3/2} + Gt\left[\frac{1-b/3}{t-(1-k_1)(1-b/3)}\right]^{3/2} + Gt\left(\frac{1-b/3}{t-1+b/3}\right)^{3/2}\right\}, \qquad (7.3)$$

$$(\Delta v)_1 = -F_k\,\frac{3B}{S(S+1)k^2}\left(M^2\left[\frac{1-b}{t-(1-k_1)(1-b)}\right] + 8Gt\left\{\left[\frac{1-b}{t-(1-k_1)(1-b)}\right]^{1/2} + \left[\frac{1-b/3}{t-(1-k_1)(1-b/3)}\right]^{1/2} + \left(\frac{1-b/3}{t-1+b/3}\right)^{1/2}\right\}\right), \qquad (7.4)$$

$$b = 0.1(k_B T_c)^{-2}\left[S^2+(S+1)^2\right](-2JSM + g\mu_B H)^2\,,$$

where k_1 is the dimensionless anisotropy constant. The calculation of α_k^a and Δv was performed on a computer by numerical methods. Taking into account that formulas (7.3) and (7.4) were obtained by expressing two-spin correlation functions through the susceptibility, and that the susceptibility was treated in terms of the molecular-field approximation, corrections for the temperature $T^1 = T_c + C/C^1(T - T_c)$ should be introduced, which makes it possible to diminish the discrepancy between the experimental and theoretical values of the susceptibility [85].

The parameters F_k and G were determined as follows. First, the dependence of $\Delta\alpha/F_k$ on H was calculated for temperatures far from T_c. This dependence has a maximum at a certain field H which is determined by the value of G. Then, F_k can be found by comparing experimental and theoretical values of $\Delta\alpha$ corresponding to the maximum. The results of the calculation for $\Delta\alpha$ and $\Delta v(H)/v(0)$ (Fig. 15) agree only qualitatively with experiment. A better agreement, as might be expected, is observed for the isotherms that were used to select F_k and G. As the temperature changes on either side of such an isotherm, the discrepancy between the theory and experiment increases. Near T_c, discrepancies between the experimental and theoretical curves occur over the entire ranges of magnetic fields and temperatures. A similar disagreement between the experimental isotherms and those calculated from the Tachiki and Maekawa's theory [85] was revealed for MnP and Tb [85, 90].

Note one more discrepancy between the theory and the experiment. It was shown that in the limit of weak fields there

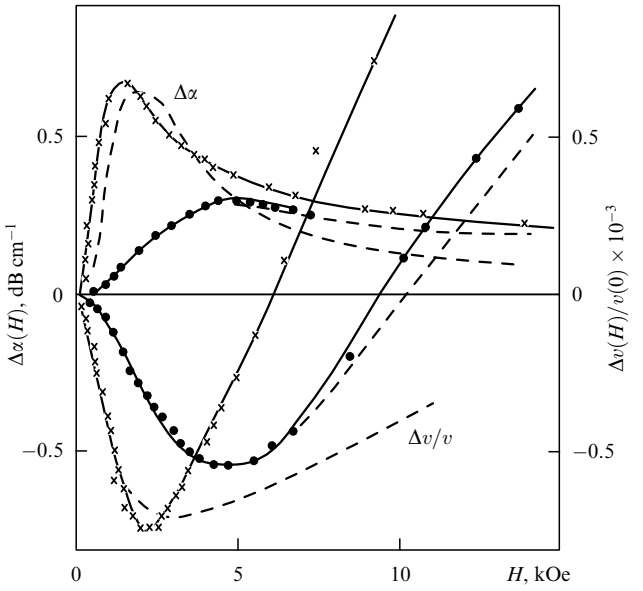

Figure 15. Experimental and theoretical dependences of $\Delta\alpha$ and $\Delta v(H)/v(0)$ on H for gadolinium at temperatures of 295.54 K (×) and 300.37 K (•); the dashed line corresponds to calculations using Eqns (7.3) and (7.4); the data points were obtained by the authors.

exists a temperature such that the contributions of the first and the other terms in Eqns (7.3) and (7.4) become equal, $\Delta\alpha = 0$ and $\Delta v(H)/v(0) = 0$ [85]. This compensation temperature depends on the difference $T_c - \Theta$ (Θ here is the paramagnetic Curie temperature) and on a constant that characterizes the range of the exchange interaction.

In magnetic insulators, including ferrimagnets, the difference $T_c - \Theta$ is large and the exchange interaction is short-range. Therefore, $\Delta\alpha$ and $\Delta v(H)/v(0)$ vanish only at very high temperatures. This result agrees qualitatively with the experiments in which the attenuation in the magnetic field was observed to decrease, i.e., in magnetic insulators the mechanism of suppression of fluctuations by a magnetic field is prevalent in the paramagnetic phase [85, 92]. However, the T_c and Θ temperatures in the metallic ferromagnets are close to one another and the compensation temperature should be close to T_c [85]. Below the compensation temperature, a magnetic field should decrease the attenuation, and above this temperature, the attenuation should increase. Our experimental data for Gd show that at all temperatures and magnetic fields, the attenuation increases in a magnetic field, which indicates the predominance of the first term in Eqn (7.3). A decrease in α_k with increasing H is only observed near T_c and only for a certain orientation of the magnetic field in the magnetically ordered phase [66].

As is seen from Fig. 13, the change in the velocity in a magnetic field passes through zero at certain values of H. With increasing T, the value of H at which $\Delta v(H)/v(0) = 0$ increases. However, the compensation temperature is independent of H and, therefore, the behavior of the velocity at $T > T_c$ appears to be related to the second term in Eqn (4.2). This part of the velocity shift plays the decisive role in a magnetic field because it behaves in the same manner as the internal energy of the spin system.

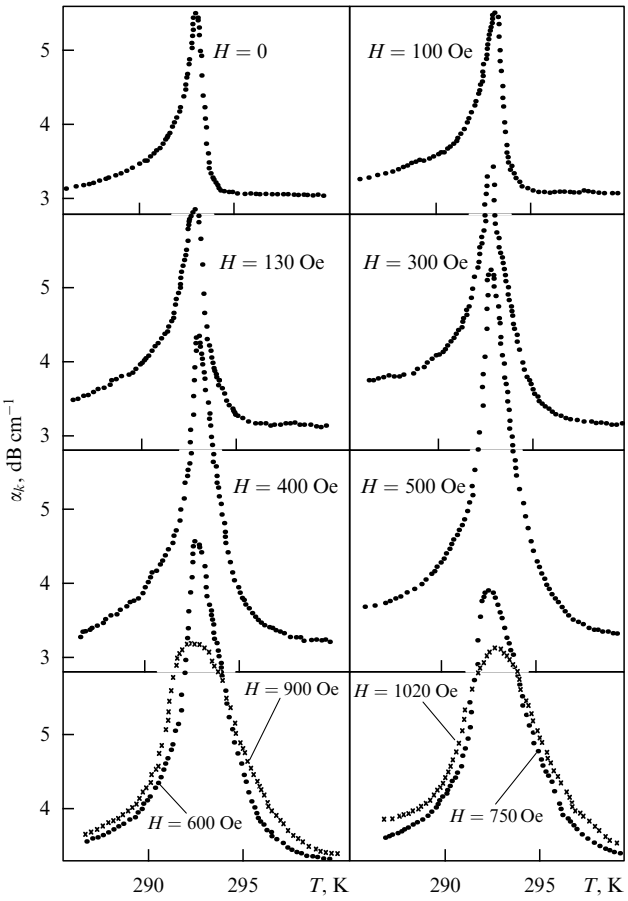

Figure 16. Temperature dependences of α_k for gadolinium in weak magnetic fields at a frequency of 15 MHz; H is perpendicular to the c axis.

7.2 Temperature dependence of the attenuation coefficient in a magnetic field

According to the general concepts [1–4], the effect of a magnetic field on the critical behavior of magnets manifests itself through the suppression of the anomalies of various physical quantities, including α_k and $\Delta v/v$. In fact, experimental studies have shown that the α_k peak shifts with increasing H toward higher temperatures and simultaneously decreases in magnitude [51]. However, in weak magnetic fields, where the polarization mechanism is predominant, such behavior is disturbed. In particular, the attenuation peak increases with increasing H [42, 69].

The curves of the temperature dependence of α_k for gadolinium for the case where the directions of the magnetic field H and the propagation direction of ultrasonic waves are mutually perpendicular are shown in Figs 16 and 17. Such an experimental geometry makes it possible to study the relaxation of the order parameter in the pure form. In all other cases, anomalies of α_k due to second-order phase transitions manifest themselves (see Ref. [66]).

As can be seen from Figs 16 and 17, the attenuation α_k near the Curie point passes through an asymmetric peak at $H = 0$. In a magnetic field, the peak value α_k increases and the $\alpha_k(T)$ curve itself becomes symmetric. With increasing H, the maximum of α_k is shifted toward lower temperatures. This shift and the increase in the peak value of α_k continue up to $H = 500-600$ Oe. A further increase in H leads to a broadening of the maximum and its displacement toward higher temperatures. An especially large shift of the maximum of α_k

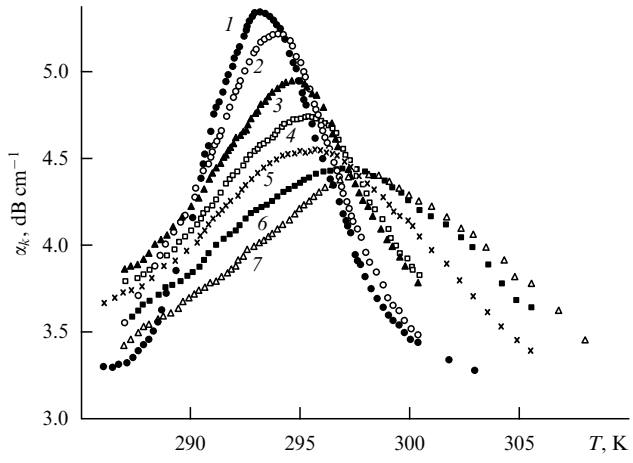

Figure 17. Temperature dependences of α_k for gadolinium in moderate magnetic fields: *1*, 1130; *2*, 1400; *3*, 1880; *4*, 2210; *5*, 3280; *6*, 3780; and *7*, 4270 Oe; H is perpendicular to the c axis.

toward higher temperatures is observed for $H > 1130$ Oe (see Fig. 17). Similar features were also revealed when H was parallel to the c axis for longitudinal waves propagating in the basal plane.

Thus, it follows from the experimental data that the behavior of the α_k maximum differs dramatically in fields $H < 600$ Oe and $H > 1130$ Oe. Let us consider the behavior of α_k and its maximum in magnetic fields below 600 Oe. Here, it

should be noted first of all that the maximum of α_k both at $H = 0$ and at $H \neq 0$ is observed in the magnetically ordered phase. In these ranges of temperatures and fields, the temperature dependences of α_k taken in different fields have much in common with the $\alpha_k(T)$ dependence at various frequencies. In both cases, an increase is observed in the peak value and a displacement of the maximum toward lower temperatures with increasing ω or H. This gives us grounds, as in the case of the $\alpha_k - \omega - T$ data, to use the theoretical concepts that follow from the Landau–Khalatnikov relaxation mechanism [7] and apply formulas (5.5)–(5.8) for the treatment of experimental data, preliminarily having replaced ω by H. The correctness of this replacement is justified by the fact that when a magnetic field is applied (e.g., perpendicular to the hexagonal axis of the crystal), there arises a Larmor precession of the uniform magnetization about the field direction with a frequency that depends linearly on H.

The dependences of $t_{\max}$ and $\alpha_{\max}$ on H represented in Fig. 18 on a double logarithmic scale confirm the validity of formulas (5.5)–(5.8). It is seen that the experimental points lie on straight lines corresponding to power laws $H \sim t_{\max}^{x}$ ($x = 1.25 \pm 0.05$) and $\alpha_{\max} \sim H^{1+y}$ ($1 + y = 0.82 \pm 0.06$). When going from $T_{\max}$ in any direction, the exponent $1 + y$ increases. For example, at $T = T_c$, we have $1 + y = 1.18 \pm 0.06$, and in the paramagnetic phase $1 + y = 2$, as was shown above. Thus, in accordance with the scaling concepts, the experimental $\alpha_k - H - T$ data can be described by a single equation by changing the scale of α_k by a factor of H^{1+y} and that of H by a factor of t^x. According to Kawasaki [19], for the relaxation mechanism the $\alpha_k - \omega - T$ data are described by Eqn (5.5). By analogy with the $\alpha_k - \omega - T$ data, we can write

$$\frac{\alpha_k}{\alpha_{\max}} = B_R \frac{At^{-x}H}{1 + A^2 t^{-2x} H^2}, \qquad (7.5)$$

where $At^{-x}H$ stands for $\omega\tau$ and A is a constant independent of T and H. This equation is justified only when the relaxation time is independent of H. The fact that τ is independent of H was shown above.

The results of the treatment of the $\alpha_k - H - T$ data using Eqn (7.5) are given in Fig. 19. Here, the dashed lines correspond to (7.5) with $x = 1.25$ and $A = 7.5 \times 10^{-6}$ for $T < T_c$, and $A = 1.25 \times 10^{-6}$ for $T > T_c$. The good correspondence of the experimental $\alpha_k - H - T$ data to Eqn (7.5) suggests that the temperature dependence of α_k in various fields H ($H < 600$ Oe) is determined by the Landau–

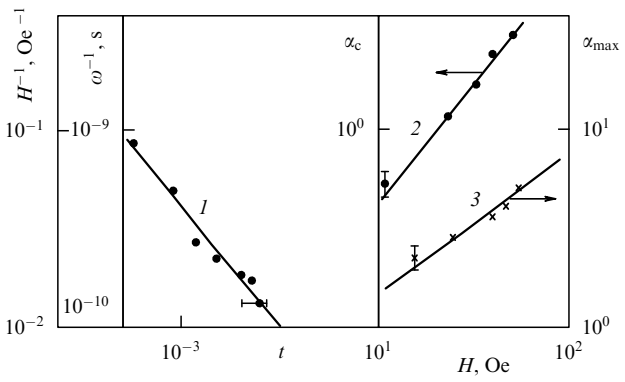

Figure 18. Dependences for Gd on a double logarithmic scale: *1*, $H^{-1}(t)$ and $\omega^{-1}(t)$; *2*, $\alpha_c(H)$, and *3*, $\alpha_{\max}(H)$.

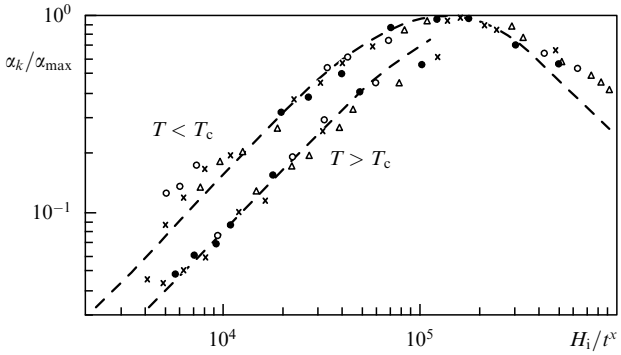

Figure 19. Scaling of attenuation at $H < 600$ Oe: •, 500; ×, 400; ○, 300; and △, 130 Oe. The dashed lines correspond to calculations using Eqn (7.5) at $x = 1.25$ and $A = 7.5 \times 10^{-6}$ for $T < T_c$, and $A = 4.06 \times 10^{-6}$ for $T > T_c$ [42].

Khalatnikov relaxation mechanism not only below but also above T_c. In this case, α_k is maximum at $\omega\tau = AHt^{-x} = 1$. This suggests that the temperature dependence τ can be found from the displacement of the maximum of α_k toward the lower temperatures with increasing H. As is seen from Fig. 18, the $H \sim t_{\max}$ dependence corresponds to the power law (4.8) with $x = 1.25 \pm 0.05$ and $\tau_0 = 2.67 \times 10^{-12}$ s. A comparison of the x and τ_0 values with the results obtained from the $\alpha_k - \omega - T$ data shows that the relaxation time in a magnetic field as $T \to T_c$ changes more strongly (see Table 4) whereas the absolute values of τ_0 undergo no significant changes. This, in turn, results in that the dynamic critical exponent $z = 1.76$ that was estimated from the relation $Z = x/\nu$ is close to the value characteristic of the normal dipolar dynamics.

In magnetic fields $H > 1130$ Oe, the appearance of a maximum of α_k in the paramagnetic phase and its shift toward higher temperatures may be caused by several mechanisms. In the presence of strong fluctuations of the order parameter near T_c, a magnetic field H greater than 1130 Oe may be regarded as strong, since the energy of the magnetic field is greater than the energy of critical fluctuations and, consequently, the long-wavelength fluctuations are suppressed by the field. As a result, the fluctuation spectrum is enriched in high frequencies, which restricts the increase of the correlation radius. Far from T_c, the magnetic field is weak and, therefore, H does not significantly affect r_c. Consequently, r_c should pass through a finite maximum at a certain temperature, which in turn leads to the appearance of a maximum in α_k. In this case, the critical exponents that characterize the field dependences of the displacements of the maximum of α_k, as well as its maximum value $\alpha_{\max}$, would be the same as for the susceptibility [42].

The treatment of the experimental data in accordance with the power relations $\alpha_{\max} \sim H^{-\lambda}$ and $T_{\max} \sim H^{\mu}$ yields values $\lambda = 0.51$ and $\mu = 1.15$, which do not correspond to the results of the fluctuation theory. Moreover, with this mechanism, α_k cannot be greater than the value of the attenuation coefficient at the corresponding temperature without a field ($H = 0$). But experiment shows that $\alpha_k(H) > \alpha_k(0)$ in the temperature range where the maximum is observed. Some improvement in the agreement between the theory and experiment can be obtained by taking into account the following specific features of the critical behavior of gadolinium. First of all, note that in a magnetic field the polarization mechanism of anomalous attenuation is opera-

tive in gadolinium, which may lead to an increase in α_k as compared to $\alpha_k(0)$ at the same temperature. In addition, the critical dynamics of gadolinium have a dipolar character (normal dipolar dynamics). If we take this into account as well as the fact that the maxima of α_k in the range of magnetic fields studied are observed at $t \leqslant 2.3 \times 10^{-2}$, i.e., at $t < t_d$, the critical exponents λ and μ are determined from the relations $\lambda = 2/z$ and $\mu = 1/x$. The first of these is a consequence of the fact that α_k is proportional to the susceptibility, and the second follows from the relation $\tau \sim r_c^z$ and the equality of the energies of the magnetic field and critical fluctuations. In either case, the values of λ and μ are calculated using the value of z for the normal dipole dynamics. Nevertheless, significant discrepancies still remain between the theory and experiment, which are not removed even if the magnetic field is corrected for the demagnetizing field. However, it should be noted that the values of λ and μ are in good agreement with the values obtained not only from the susceptibility [66] but also from the attenuation of ultrasonic waves in MnP [51].

According to the scaling hypothesis, the $\alpha_k - H - T$ data can be described by a single equation by changing the scale of α by a factor of $H^{-\lambda}$ and that of t by a factor of H^{μ}. Then,

$$\frac{\alpha_k}{\alpha_{\max}} = B\,\frac{2AtH^{-1.15}}{1 + A^2t^2H^{-2.30}}\,. \tag{7.6}$$

The results of the treatment of experimental data by Eqn (7.6) are shown in Fig. 20. Here, the solid line represents Eqn (7.6) with $A = 1.47 \times 10^{-6}$ and $\mu = 1.15$ and the data points denoted by different signs correspond to experimental data at different values of H. From the form of this scaling equation, it follows that the maximum of $\alpha_k/\alpha_{\max}$ will be observed at $At/H^{1.15} = 1$, which corresponds to the condition $\omega\tau = 1$ for the relaxation mechanism of the anomalous attenuation of ultrasonic waves. From the condition for a maximum, it follows that the relaxation time at a constant temperature decreases in a magnetic field according to the law $T \sim H^{-1.15}$, and at a constant field it increases linearly with increasing temperature. The first result agrees with the predictions of Kawasaki [8] and Halperin and Hohenberg [10, 12] for the diffusional decay of fluctuations, according to which $\tau \sim H^{-1}$. The second result may be due to the manifestation of the Huber attenuation [93] in a magnetic field, for which $\tau \sim t$. The appearance of the Huber attenuation in the dipolar region in a magnetic field, which usually is observed in the exchange region, may be related to the fact that with the application of a magnetic field H, the susceptibility decreases. Consequently, in a strong magnetic field almost the entire temperature range below $T_{\max}$ corresponds to exchange interactions, and dipolar interactions in this case may be considered as small perturbations [13]. However, at $T = T_{\max}$ in the magnetic-field range studied we have $\chi \geqslant 1$ and, therefore, the dipolar forces cannot be considered as a small perturbation. Thereby, at $T = T_{\max}$, a crossover occurs from dipole to exchange behavior. This may explain the discrepancy between the experimental values of μ and the theory.

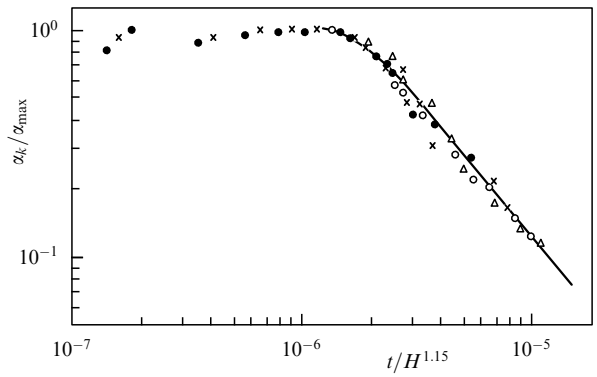

Figure 20. Scaling of attenuation at $H > 1160$ Oe: △, 1880; ○ 3280; ×, 3780; and •, 4270 Oe.

Note also that the quadratic dependence of $\Delta\alpha$ and Δv on H predicted by the polarization mechanism follows from the assumption of the proportionality of the magnetization to the field H, which, as experimental studies show [66], is not fulfilled over almost the whole temperature range and especially near T_c. The quadratic field dependence of $\Delta\alpha$ and Δv follows from the relaxation of the uniform magnetization. With the linear relation between the sound waves and the order parameter, we have, according to Kawasaki [19],

$$\alpha_R(\omega) = r_c^{2/\nu-3}\omega f(r_c^z\omega)\,. \tag{7.7}$$

Hence, at $r_c^z\omega \ll 1$, we have $\alpha_R(\omega) \sim \omega^2 r_c^{2/\nu-3+z}$, since in this case $f(x) \approx x$. In a weak field, the correlation radius is independent of the magnetic field [13] and, therefore, the field dependence of α_k is determined by the frequency ω (by ω, we should mean the frequency of the Larmor precession), which, as is known, is proportional to the strength of the magnetic field H.

Thus, the specific features of the field and temperature dependences of $\Delta\alpha$ and $\Delta v(H)/v(0)$ can be explained using two mechanisms of anomalous attenuation of ultrasonic waves — relaxational and fluctuational. As to the polarization mechanism, it, in our opinion, does not differ in any features from the relaxation mechanism, since both mechanisms are based on the same linear relation between the sound waves and the order parameter.

8. Conclusions

Thus, we see that studying critical dynamics by ultrasonic methods has its own features in magnetically ordered crystals depending on the character of the exchange interaction. Depending on the range of the ordering interaction, the sound waves interact with either fluctuations of the spin-energy density (magnetic insulators) or fluctuations of the order parameter (magnetic metals). In the first case, the decay of fluctuations occurs by slow spin–lattice relaxation, which is known to exhibit a weak singularity ($x = \alpha$). In this connection, the success of the determination of the critical exponent z from ultrasonic experiments using the relation $x = z\nu$ is problematic. In magnetic metals with a long-range exchange interaction, the decay of fluctuations of the order parameter occurs through spin–spin relaxation, which exhibits a much stronger singularity ($x = 1 - 5/3$) as compared to the spin–lattice relaxation. In this case it is possible to define the dynamic critical index z from ultrasonic experiments.

Acknowledgments
We are grateful to A S Borovik-Romanov, I M Khalatnikov, and K P Belov for their interest in our work and fruitful discussions.

References

1. Landau L D, Lifshitz E M *Statisticheskaya Fizika* (Statistical Physics) (Moscow: Nauka, 1976) [Translated into English (Oxford: Pergamon Press, 1980)]
2. Patashinskiĭ A Z, Pokrovskiĭ V L *Fluktuatsionnaya Teoriya Fazovykh Perekhodov* (Fluctuation Theory of Phase Transitions) (Moscow: Nauka, 1982) p. 9 [Translated into English (Oxford: Pergamon Press, 1979)]
3. Stanley H E *Introduction to Phase Transitions and Critical Phenomena* (Oxford: Clarendon Press, 1971) [Translated into Russian (Moscow: Mir, 1973)]
4. Ma Sh *Modern Theory of Critical Phenomena* (London: W.A. Benjamin Inc., 1976) [Translated into Russian (Moscow: Mir, 1980)]
5. Anisimov M A *Kriticheskie Yavleniya v Zhidkostyakh i Gazakh* (Critical Phenomena in Liquids and Gases) (Moscow: Nauka, 1987) p. 7
6. Kamilov I K, Aliev Kh K *Staticheskie Kriticheskie Yavleniya v Magnitouporyadochennykh Kristallakh* (Static Critical Phenomena in Magnetically Ordered Crystals) (Makhachkala: Dagestan. Nauchn. Tsentr, Ross. Akad. Nauk, 1993) p. 7
7. Landau L D, Khalatnikov I M *Dokl. Akad. Nauk SSSR* **96** 469 (1954)
8. Kawasaki K, in *Critical Phenomena. Proc. Int. School Phys. "Enrico Fermi"* Course 51 (New York: Acad. Press, 1971) [Translated into Russian (Moscow: Mir, 1975) p. 101]
9. Kadanoff L P, Swift J *Phys. Rev.* **166** 89 (1968)
10. Halperin B I, Hohenberg P C *Phys. Rev.* **177** 952 (1969)
11. Wilson K, Kogut J "The renormalization group and the ε expansion" *Phys. Rep.* **12** 75 (1974) [Translated into Russian (Moscow: Mir, 1972)]
12. Hohenberg P C, Halperin B I *Rev. Mod. Phys.* **49** 435 (1977)
13. Maleev S V, Preprint LIYaF No. 1038 (Leningrad: LIYaF, 1985)
14. Maleev S V, Preprint LIYaF No. 1039 (Leningrad: LIYaF, 1985)
15. Maleev S V, Preprint LIYaF No. 1040 (Leningrad: LIYaF, 1985)
16. Teitel'baum G B *Pis'ma Zh. Eksp. Teor. Fiz.* **21** 339 (1975) [*JETP Lett.* **21** 154 (1975)]
17. Tani K, Mori H *Prog. Theor. Phys.* **39** 876 (1968)
18. Lüthi B, Moran T J, Pollina R J *J. Phys. Chem. Solids* **31** 1741 (1970)
19. Kawasaki K, in *Proc. Conf. Internal Friction and Ultrasonic Attenuation in Solids* (Tokyo: Tokyo University Press, 1977) p. 29
20. Kawasaki K *Phys. Lett. A* **29** 406 (1969)
21. Gorodetsky G, Luthi B, Moran T J *Inter. J. Magn.* **1** 295 (1971)
22. Kawasaki K *Phys. Lett. A* **26** 543 (1968)
23. Laramore G E, Kadanoff L P *Phys. Rev.* **187** 619 (1969)
24. Golding B, Barmatz M *Phys. Rev. Lett.* **23** 223 (1969)
25. Basu B K *Phys. Status Solidi* **38** 857 (1970)
26. Basu B K *Phys. Status Solidi B* **45** K95 (1971)
27. Golding B *Phys. Rev. Lett.* **34** 1102 (1975)
28. Suzuki M *J. Phys. Soc. Jpn.* **50** 1149 (1981)
29. Suzuki M, Kato K, Ikeda H *J. Phys. Soc. Jpn.* **49** 514 (1980)
30. Suzuki M, Kato K, Ikeda H *J. Phys. Soc. Jpn.* **49** 1323 (1980)
31. Suzuki M, Komatsubara T *J. Phys. C* **15** 4559 (1982)
32. Kamilov I K, Aliev Kh K *Pis'ma Zh. Eksp. Teor. Fiz.* **15** 715 (1972) [*JETP Lett.* **15** 506 (1972)]
33. Kamilov I K, Aliev Kh K *Zh. Eksp. Teor. Fiz.* **65** 1911 (1973) [*Sov. Phys. JETP* **38** 954 (1974)]
34. Kamilov I K, Aliev Kh K *Fiz. Tverd. Tela* (Leningrad) **12** 1855 (1970)
35. Kamilov I K, Aliev Kh K *Khimicheskaya Svyaz' v Poluprovodnikakh i Polumetallakh* (Chemical Bond in Semiconductors and Semimetals) (Minsk: Nauka i Tekhnika, 1974) p. 367
36. Kamilov I K et al. *Struktura i Svoĭstva Ferritov* (Structure and Properties of Ferrites) (Minsk: Nauka i Tekhnika, 1974) p. 73
37. Kamilov I K et al. *Zh. Eksp. Teor. Fiz.* **68** 2290 (1975) [*Sov. Phys. JETP* **41** 1144 (1976)]
38. Kamilov I K et al. *Zh. Eksp. Teor. Fiz.* **68** 586 (1975) [*Sov. Phys. JETP* **41** 290 (1975)]
39. Kamilov I K et al. *Teplofizicheskie Svoĭstva Tverdykh Tel* (Thermophysical Properties of Solids) (Kiev: Naukova Dumka, 1971) p. 192
40. Kamilov I K, Aliev Kh K, Shakhshaev G M *Fiz. Tverd. Tela* (Leningrad) **15** 914 (1973)
41. Kamilov I K et al. *Tez. dokl. 17 Vsesouznoi Konferentsii po Fizike Magnitnykh Yavleniĭ* (17th All-Union Conf. on Magnetic Phenomena, Abstracts of Papers) (Donetsk: Naukova Dumka, 1985) p. 105
42. Aliev Kh K, Doctoral (Phys.-Math.) Dissertation (Moscow: Moscow State University, 1996)
43. Kawasaki K, Ikushima A *Phys. Rev. B* **1** 3143 (1970)
44. Bloch D *J. Phys. Chem. Solids* **27** 881 (1966)
45. Samara G A, Giardini A A *Phys. Rev.* **186** 577 (1969)
46. Dolejsi D A, Swenson C A *Phys. Rev. B* **24** 6326 (1981)
47. Lüthi B, Pollina R J *Phys. Rev.* **167** 488 (1968)
48. Nikitin S A *Magnitnye Svoĭstva Redkozemel'nykh Metallov i Splavov* (Magnetic Properties of Rare-Earth Metals and Alloys) (Moscow: MGU, 1989); Pollina R J, Lüthi B *Phys. Rev.* **177** 841 (1969)
49. Andreeva L P, Zinov'eva G P, Gel'd P V *Fiz. Tverd. Tela* (Leningrad) **13** 3435 (1971)
50. Anikeev D I et al. *Fiz. Met. Metalloved.* **55** 622 (1983)
51. Ishizaki A et al., in *Proc. Int. Conf. Magn.* ICM-73 Vol. 3 (Moscow: Nauka, 1974) p. 208
52. Neighbours J R, Moss R W *Phys. Rev.* **173** 542 (1968)
53. Leisure R G, Moss R W *Phys. Rev.* **188** 840 (1969)
54. Ikushima A *J. Phys. Chem. Solids* **31** 939 (1970)
55. Moran T J, Lüthi B *Phys. Rev. B* **4** 122 (1971)
56. Bachellerie A, Joffrin J, Levelut A *Phys. Rev. Lett.* **30** 617 (1973)
57. Golding B *Phys. Rev. Lett.* **20** 5 (1968)
58. Moran T J, Lüthi B *J. Phys. Chem. Solids* **31** 1735 (1970)
59. Goncharov K V, Mal'tseva I V, Savitskiĭ E M *Fiz. Tverd. Tela* (Leningrad) **13** 3700 (1971)
60. Tachiki M et al. *Phys. Rev. Lett.* **34** 1579 (1975)
61. Maekawa S, Takahashi S, Tachiki M *Prog. Theor. Phys.* **59** 23 (1978)
62. Golding B et al. *Phys. Rev. Lett.* **30** 968 (1973)
63. Aliev Kh K et al. *Zh. Eksp. Teor. Fiz.* **79** 902 (1980) [*Sov Phys. JETP* **52** 458 (1980)]
64. Belov K P, Shebaldin N V *Pis'ma Zh. Eksp. Teor. Fiz.* **7** 268 (1968) [*JETP Lett.* **7** 208 (1968)]
65. Drabkin G M et al. *Pis'ma Zh. Eksp. Teor. Fiz.* **15** 379 (1972) [*JETP Lett.* **15** 267 (1972)]
66. Kamilov I K, Aliev Kh K *Usp. Fiz. Nauk* **140** 639 (1983) [*Sov. Phys. Usp.* **26** 696 (1983)]
67. Walther K *Solid State Commun.* **5** 399 (1967)
68. Lemanov V V, Pavlenko A V *Zh. Eksp. Teor. Fiz.* **57** 1528 (1969) [*Sov. Phys. JETP* **30** 826 (1970)]
69. Long M, Stern R *Phys. Rev. B* **4** 4094 (1971)
70. Kashceev V N *Phys. Lett. A* **25** 71 (1967)
71. Bennett H S *Phys. Rev.* **185** 801 (1969)
72. Huber D L *Phys. Rev. B* **3** 836 (1971)
73. Itoh Y *J. Phys. Soc. Jpn.* **38** 336 (1975)
74. Bennett H S, Pytte E *Phys. Rev.* **155** 553 (1967)
75. Pytte E, Bennett H S *Phys. Rev.* **164** 712 (1967)
76. Bennett H S *Phys. Rev.* **181** 978 (1969)
77. Pokrovskiĭ V L, Khalatnikov I M *Pis'ma Zh. Eksp. Teor. Fiz.* **9** 255 (1969) [*JETP Lett.* **9** 149 (1969)]
78. Aliev Kh K, Kamilov I K, Omarov A M *Zh. Eksp. Teor. Fiz.* **94** 153 (1988) [*Sov. Phys. JETP* **67** 2262 (1988)]
79. Chowdhury A R, Collins G S, Hohenemser C *Phys. Rev. B* **30** 6277 (1984)
80. Burgardt P, Seehra M S *Phys. Rev. B* **16** 1802 (1977)
81. Collins G S, Chowdhury A R, Hohenemser C *Phys. Rev. B* **33** 4747 (1986)
82. Chowdhury A R, Collins G S, Hohenemser C *Phys. Rev. B* **33** 5070 (1986)
83. Aliev Kh K et al. *Zh. Eksp. Teor. Fiz.* **95** 1896 (1989) [*Sov. Phys. JETP* **68** 1096 (1989)]
84. Belov K P, Kataev G I, Levitin R Z *Zh. Eksp. Teor. Fiz.* **37** 938 (1959) [*Sov. Phys. JETP* **37** 670 (1960)]
85. Tachiki M, Maekawa S *Prog. Theor. Phys.* **51** 1 (1974)
86. Tachiki M, Lee M C, Levy M *Phys. Rev. Lett.* **29** 488 (1972)
87. Vigren D T *Phys. Rev. Lett.* **38** 1155 (1977)
88. Maekawa S, Tachiki M *Phys. Rev. B* **18** 3736 (1978)
89. Aliev Kh K et al. *Fiz. Tverd. Tela* (Leningrad) **26** 265 (1984)
90. Maekawa S et al. *Phys. Rev. B* **13** 1284 (1976)
91. Aliev Kh K, Kamilov I K, Magomedgadzhiev Kh I *Fiz. Tverd. Tela* (Leningrad) **23** 1533 (1981)
92. Neighbours J R, Oliver R W, Stillwell C H *Phys. Rev. Lett.* **11** 125 (1963)
93. Huber D L *J. Phys. Chem. Solids* **32** 2145 (1971)
94. Glinka C J, Minkiewicz V J, Passell L *Phys. Rev. B* **16** 4084 (1977)
95. Hohenemser C, Chow L, Sufer R M *Phys. Rev. A* **22** 5056 (1982)
96. Kobeissi M A *Phys. Rev. B* **24** 2380 (1981)
97. Riedel E K *J. Appl. Phys.* **42** 1383 (1971)
98. Bucci C, Guidi G, Vidnali C *Solid State Commun.* **10** 803 (1972)